*Science in China Series D: Earth Sciences*



www.scichina.com
earth.scichina.com
www.springerlink.com

# Conditional nonlinear optimal perturbation: Applications to stability, sensitivity, and predictability

DUAN WanSuo & MU Mu†

State Key Laboratory of Numerical Modeling for Atmospheric Sciences and Geophysical Fluid Dynamics, Institute of Atmospheric Physics, Chinese Academy of Sciences，Beijing 100029, China

**Conditional nonlinear optimal perturbation (CNOP) is a nonlinear generalization of linear singular vector (LSV) and features the largest nonlinear evolution at prediction time for the initial perturbations in a given constraint. It was proposed initially for predicting the limitation of predictability of weather or climate. Then CNOP has been applied to the studies of the problems related to predictability for weather and climate. In this paper, we focus on reviewing the recent advances of CNOP's applications，which involves the ones of CNOP in problems of ENSO amplitude asymmetry, block onset, and the sensitivity analysis of ecosystem and ocean's circulations, etc. Especially, CNOP has been primarily used to construct the initial perturbation fields of ensemble forecasting, and to determine the sensitive area of target observation for precipitations. These works extend CNOP's applications to investigating the nonlinear dynamical behaviors of atmospheric or oceanic systems, even a coupled system, and studying the problem of the transition between the equilibrium states. These contributions not only attack the particular physical problems, but also show the superiority of CNOP to LSV in revealing the effect of nonlinear physical processes. Consequently, CNOP represents the optimal precursors for a weather or climate event; in predictability studies, CNOP stands for the initial error that has the largest negative effect on prediction; and in sensitivity analysis, CNOP is the most unstable (sensitive) mode. In multi-equilibrium state regime, CNOP is the initial perturbation that induces the transition between equilibriums most probably. Furthermore, CNOP has been used to construct ensemble perturbation fields in ensemble forecast studies and to identify sensitive area of target observation. CNOP theory has become more and more substantial. It is expected that CNOP also serves to improve the predictability of the realistic predictions for weather and climate events plays an increasingly important role in exploring the nonlinear dynamics of atmospheric, oceanic and coupled atmosphere-ocean system.**

optimal perturbation, predictability, stability, sensitivity

One of the central problems in atmospheric and oceanic sciences is the predictability for weather and climate, in which estimating the prediction uncertainty is very important. Tennekes[1] proclaimed that no forecast was complete without an estimate of the prediction error. This perspective can be traced back to Thompson[2]. Since then, operational weather forecasting has progressed to the point of explicit attempts to quantifying the evolution of initial uncertainty during each forecast[3−5], which, furthermore, has been permeated through coupled model forecasts. Some understandings of the predictability of the tropical ocean-atmosphere system have been gained by studying the growth of errors and uncertainties during forecasts[6−10].

Despite the consensus on the best approach for predicting large dynamical systems like the Earth's atmos-

Received December 8, 2008; accepted April 27, 2009
doi: 10.1007/s11430-009-0090-3
†Corresponding author (email: mumu@lasg.iap.ac.cn)
Supported by National Basic Research Program of China (Grant Nos. 2006CB403606, 2007CB411800), National Natural Science Foundation of China (Grant Nos. 40830955, 40675030, 40505013), Institute of Atmospheric Physics, Chinese Academy of Sciences (Grant No. IAP07202), and LASG State Key Laboratory Special Fund

**Citation:** Duan W S, Mu M. Conditional nonlinear optimal perturbation: Applications to stability, sensitivity, and predictability. Sci China Ser D-Earth Sci, 2009, 52(7): 883-906, doi: 10.1007/s11430-009-0090-3

phere, optimal methods for quantifying the evolution of uncertainty remain the subject of debate[11]. One of the approaches based on optimal growth is linear singular vector (LSV), which, first introduced by Lorenz[12], is established on the basis that the evolution of initial perturbation can be described approximately by the tangent linear model (TLM). LSV approach has been widely used to tackle the problems related to error growth predictability[7,13]. As an extension of LSV applications, it was also used to the studies of atmospheric and oceanic dynamics[14−16]. However, due to the absence of nonlinearity, LSV has limitations in describing the nonlinear optimal growth of the finite amplitude initial perturbations. Since the motions of atmospheric and oceanic flows are generally nonlinear, LSV could not guarantee the role of initial uncertainties having the largest effect on prediction results, whereas it is the fastest-growing perturbation in TLM[17,18].

To study the effect of nonlinearity, Mu[17] and Mu and Wang[19] directly used nonlinear models and proposed the concepts of nonlinear singular vector (NLSV) and nonlinear singular value (NSVA). They demonstrated that for some types of basic flows in numerical models, there exist not only the first NLSVs, but also local fastest-growing perturbations, at which the objective function attains the local maximums. Nevertheless, this phenomenon does not occur in LSV approach. Furthermore, Mu and Wang[19] showed that those local fastest-growing perturbations are usually of larger norms than the first NLSVs; although the growth rates of the local fastest-growing perturbations are smaller than those of the first NSVAs, their nonlinear evolutions at the end of the time interval are considerably greater than those of the first NLSVs. In this case, the local fastest growing perturbations could play a more important role than the global fastest growing perturbation (first NLSV) in the study of the predictability. Apparently, to explore the initial uncertainty that has the severest negative effect on prediction results, one should first find out all local fastest growing perturbations, compare their impacts on the predictability, and then seek the optimal initial perturbation related to the largest effect on the predictability. This is very inconvenient in applications. Besides, such perturbations could be physically unreasonable because of large amplitude of norm. For example, since the observed sea surface temperature anomaly (SSTA) does not exceed 6℃, the physically reasonable SSTA in optimal perturbations should not be larger than 6℃; however, a local fastest-growing perturbation related to SSTA with large amplitude may exceed this bound of 6℃; in this case, such local fastest-growing perturbation does not make sense in physics.

As mentioned above, NLSV approach has several limitations; LSV cannot reveal effectively the nonlinear effect. It is therefore necessary to develop a more useful tool that can not only consider the nonlinear effect, but also overcome the limitations of NLSV. Upon this request, Mu et al.[18] proposed a novel approach of conditional nonlinear optimal perturbation (CNOP). CNOP is different from NLSV and describes the initial perturbation that has the largest nonlinear evolution at prediction time. The property of the fastest growth of LSV lies in the measurement of the linear growth rate of the initial perturbations, whereas CNOP is measured by the nonlinear evolution at prediction time. The essence of CNOP's maximum nonlinear evolution is to make it represent the initial uncertainties that has the largest impact on forecast results and play a more important role than NLSV and LSV in the predictability studies[20,21].

CNOP has first been applied in ENSO predictability to find the optimal precursor of ENSO events[22] and to explore the spring predictability barrier (SPB)[9]. Then the application was extended to the stability and sensitivity analysis of thermohaline circulation (THC)[23,24]. All these works demonstrated the differences between CNOP and LSV for the finite amplitude of initial perturbations and/or the long time intervals[5,18], and revealed the role of nonlinear physical processes in stability, sensitivity, and predictability studies. However, these results are all based on theoretical models.

Recently, CNOP theory has been more complete. Furthermore, some new applications in atmospheric and oceanic sciences show the usefulness of CNOP in the dynamics studies of atmosphere, ocean, and coupled systems besides the fields of stability, sensitivity, and predictability. For example, Liu[25] proved theoretically that CNOPs locate at the boundary of a given constraint, which coincides with the numerical results demonstrated by other papers[5,18]. Riviere et al.[26] applied CNOP-like approach in a two-layer quasi-geostrophic model of baroclinic instability to investigate the effect of nonlinearities on the behavior of baroclinic unstable flows. Terwisscha van Scheltinga[27] computed the CNOPs of the double-gyre ocean circulation by an implicit 4D-Var

methodology and studied the finite amplitude stability of the double-gyre flow. In particular, CNOP approach has been used in the studies of ensemble forecast and adaptive observation (see section 5). These studies not only extend the applications of CNOP, but also reveal more physics of CNOP and make CNOP theory more substantial.

In this paper, we will review CNOP idea and its recent applications. In section 1, the definition of CNOP and its computation and physical meanings are reviewed. From sections 2 to 4, we will take the physical meanings of CNOP as a syllabus to introduce the recent applications of CNOP in stability, sensitivity, and predictability for weather and climate. For example, for the physics of CNOP as optimal precursor for a weather or climate events, the applications of CNOP to blocking onset and ENSO asymmetry is introduced in section 2; in section 3, the application of CNOP in the SPB for ENSO events is reviewed with CNOP as the initial error that has the largest effect on predictions; in section 4, CNOP's application is extended to the sensitivity and stability analysis of baroclinic unstable flow, ocean's circulation and ecosystem within the physics of CNOP as the most unstable mode. Besides, reviewed in section 5 is a novel application of CNOP in constructing ensemble initial perturbations and target observation. Finally, section 6 summarizes the main properties of CNOP and the differences between CNOP and LSV based on the works reviewed in previous sections. In addition, section 6 also discusses some potential applications in the future.

## 1 Conditional nonlinear optimal perturbation

CNOP is a new method to tackle optimal growth problems of perturbation, and is different from the widely-used LSV approach in predictability and dynamics studies. When nonlinearities in a numerical model begin to be active, CNOP method plays an important role in describing the nonlinear effect. Therefore, CNOP method could be a useful tool in studying the predictability of nonlinear atmosphere, ocean, and coupled system. In exploring their nonlinear dynamics, CNOP may also be an important approach, as shown in latter sections.

### 1.1 Definition of CNOP

Let $M_t$ be a propagator (i.e., numerical model) of a nonlinear model, which propagates the initial value to the future time *t*. $u_0$ is an initial perturbation superposed on a basic state $U(t)$, which is a numerical solution to the nonlinear model and satisfies $U(t)=M_t(U_0)$ at time $t$ ($U_0$ is the initial value of $U(t)$). Then

$$U(t)+u(t)=M_t(U_0+u_0), \tag{1}$$

so $u(t)$ describes the evolution of the initial perturbation $u_0$.

For a chosen norm $\|\cdot\|$, an initial perturbation $u_{0\delta}$ is called CNOP, if and only if $J(u_{0\delta})=\max_{\|u_0\|\leqslant\delta} J(u_0)$, where

$$J(u_0)=\left\|M_\tau(U_0+u_0)-M_\tau(U_0)\right\|, \tag{2}$$

$\|u_0\|\leqslant\delta$ is the initial constraint defined by the chosen norm $\|\cdot\|$. The norm $\|\cdot\|$ also measures the evolution of the perturbations. Here, the constraint condition is simply expressed as belonging to a ball with the chosen norm. Obviously, we can also investigate the situation that the initial perturbations belong to other kind of functional set. Furthermore, the constraint condition could be some physical laws that initial perturbation should satisfy.

Mathematically, CNOP is the global maximum of $J(u_0)$ over the ball $\|u_0\|\leqslant\delta$[5,18]. It is also possible that there exist local maximum value of $J(u_0)$. In this case, we call the corresponding maximum as a local CNOP.

From eq. (2), it is easily seen that CNOP is defined by using directly the nonlinear model, which is therefore different from LSV. LSV is based on a TLM and represents the fastest-growing perturbation in TLM. Let $M$ be the TLM of $M_t$, then LSV can be obtained by solving

$$\lambda=\max_{u_0}\frac{\|M(U_0+u_0)-M(U_0)\|}{\|u_0\|}=\max_{u_0}\frac{\|M(u_0)\|}{\|u_0\|}, \tag{3}$$

where $\lambda$ is linear singular value (i.e. the growth rate of LSV). The tangent linear operator, $M$, is a matrix. According to the matrix theory, eq. (3) can be rewritten as

$$\lambda=\frac{\lambda_{\max}\|u_0^*\|}{\|u_0^*\|}, \tag{4}$$

where $u_0^*$ is the first LSV, $\lambda_{\max}$ is the positive square root of the largest eigenvalue of the symmetric matrix $M^*M$ ($M^*$ is the adjoint matrix of $M$). From eq. (4), we can derive that for any constant $c$, the vector $cu_0^*$ is also a LSV. Furthermore, for different $c$, the LSVs $cu_0^*$ correspond to the same singular value. Therefore, LSV

represent the direction of the fastest growth of initial perturbations.

LSV is established on that initial perturbations are sufficient small such that the corresponding TLM can describe their evolutions. However, CNOP, since it considers the effect of nonlinearity, is not affected by this limitation and can explore the development of finite amplitude perturbations. It is conceivable that when the initial constraint is very small, CNOP could be approximated by LSV; when initial perturbations are large, LSV's approximation to CNOP does not hold. In this case, CNOP, due to the nonlinearity, does not represent the direction of the fastest growing of initial perturbations, but a kind of perturbations that have the largest nonlinear evolution at prediction time. CNOP is superior to LSV in revealing the nonlinear effect.

### 1.2 Computation of CNOP

CNOP can be computed by some ready solvers such as the sequential quadratic programming (SQP) and the Spectral Projected Gradient 2 (SPG2), which are used to solve the nonlinear minimization problems with equality or/and inequality constraint condition[28,29].

Let

$$J_1(u_0) = -\frac{1}{2}[J(u_0)]^2. \tag{5}$$

Eq. (2) becomes a minimum problem

$$J_1(u_{0\delta}) = \min_{\|u_0\| \leqslant \delta} J_1(u_0). \tag{6}$$

In SQP and SPG2 algorithms, the gradient of $J_1(u_0)$ with respect to $u_0$ is required, where the adjoint method is a useful tool in computing the gradient of the function related to model solutions. The gradient of $J_1(u_0)$ with respect to $u_0$ is as follows:

$$\nabla J_1(u_0) = -M^*_\tau(U_0 + u_0)(M_\tau(U_0 + u_0) - M_\tau(U_0)), \tag{7}$$

where $M^*_\tau(U_0 + u_0)$ is the adjoint propagator of the TLM $M_\tau(U_0 + u_0)$ at $U_0$+$u_0$. By applying this gradient information in the above solvers, CNOPs can be calculated numerically.

Sometimes, CNOP can also be computed by transferring eq. (2) into another minimum problem, i.e.,

$$J_2(u_0) = \frac{1}{2[J(u_0)]^2},$$

$$J_2(u_{0\delta}) = \min_{\|u_0\| \leqslant \delta} J_2(u_0). \tag{8}$$

However, there exists possibility that $J(u_0)$ is zero at some optimization iterations. In this situation, $J_2(u_0)$ is unmeaning. The optimization algorithm cannot output a reasonable result. It is therefore suggested that one adopts the minimum problem shown in eq. (6) to compute CNOPs.

Mu et al.[18], Duan et al.[22], and Mu et al.[23], etc. used simple models consisting of a set of ordinary differential equations (ODEs) and solved numerically the CNOP by a SQP solver. Some common characteristics of CNOP were found. First, when linear approximation is not valid, CNOP is significantly different from LSV. Second, in some cases, there exist local CNOPs with clear physical meaning. Third, all the CNOPs and local CNOPs locate on the boundary of the domain defined by the given constraint condition in phase space.

To examine whether or not the above properties of CNOP hold in more complex models consisting of partial differential equations, Mu and Zhang[5] employed a two-dimensional quasigeostrophic model to compute the CNOPs. Then the obtained CNOPs also have above three characteristics. Furthermore, Jiang et al.[30], through a three-level global quasi-geostrophic (QG) spectral model, demonstrated that the patterns of CNOPs depend on the choice of the measurement norm.

Especially, Liu[25] proved theoretically the third characteristic of CNOP, that is, all CNOPs locate on the boundary of initial constraint. This contribution further establishes the inherence of the above third property for CNOPs and provides a theoretical basis for reducing the computation of CNOP. To facilitate the readers, we introduce the details.

Without loss of generality, $u_0$ in eq. (1) is assumed as the initial perturbation of the origin and its development is governed by a numerical model $M_t'$, i.e., $u(t) = M_t'(u_0)$, where the origin is regarded as the basic state and when $u_0$=0, $u(t)$=0 (i.e., the origin is assumed to be an equilibrium basic state). Then the optimization problem related to CNOP becomes

$$J(u_{0\delta}) = \max_{\|u_0\| \leqslant \delta} \| u(T; u_0) \|. \tag{9}$$

In eq. (9), $\|u_0\| \leqslant \delta$ is the constraint. Denote the set determined by $|u_0| \leqslant \delta$ as $Q$, then $Q$ is a closed set including the origin, which indicates that the initial value of $M_t'$ related to CNOP is constrained by the set $Q$. Besides, it is further assumed that the numerical model $M_t'$ here is well-defined and for a finite time $T$, the

solutions $u(T)$ have an upper bound, that is, the solutions $u(T)$ belongs to a closed set, denoted as $S$. Let $q_T$ be one of such solutions. Assume that

**(R1)** for any initial perturbation $u_0$ in $Q$, there exists a unique solution $u(t; u_0)$ of $M_t'$, which, furthermore, depends continuously on the initial value $u_0$. Denote the set of all the solutions $u(T; u_0)$ (with initial values $u_0$ in $Q$) as $P$, then $P$ is included in the constraint $S$.

**(R2)** for any $q_T$ in $S$, there exists a unique initial value $q(t, q_0)$ of $M_t'$. This initial value depends continuously on $q_T$.

Suppose that $u_{0\delta}$ is a CNOP, and $u_{\delta T}$ is the solution caused by it (i.e., the evolution of $u_{0\delta}$). It is easily shown that if $J(u_{0\delta})=0$, then $u(T; u_0)=0$ for any $u_0$ in $Q$. From the assumption (R2), this phenomenon is unreasonable. Therefore, $J(u_{0\delta})>0$ holds. Suppose that the CNOP does not locate the boundary of the initial constraint $Q$, but the interior of $Q$. From (R1) and (R2), it can be derived that for a sufficiently small $\varepsilon > 0$, the perturbation $u_0^{\varepsilon} = (1+\varepsilon)u_{0\delta}$ also locate the interior of $Q$ and $q_T^{\varepsilon} = (1+\varepsilon)u_{\delta T}$ is an interior point of $S$. It follows that for sufficiently small $\varepsilon > 0$, the initial value of the solution $q_T^{\varepsilon} = (1+\varepsilon)u_{\delta T}$, $q(0; q_T)$, is an interior point of $Q$. Consequently, for $u(t)= M_t'(u_0)$, when $u_0=q(0; q_T)$, the solution caused by $u_0$ satisfies $u(T; u_0)= M_t'(u_0)= q_T^{\varepsilon} = (1+\varepsilon)u_{\delta T}$. Then it is obtained that

$$J(u_0) - J(u_{0\delta}) = \| (1+\varepsilon)u_{\delta T} \| - \| u_{\delta T} \| > 0. \quad (10)$$

However, $u_{0\delta}$ is assumed to be CNOP. The objective function $J$ attains the maximum. The expression $J(u_0)-J(u_{0\delta})<0$, which is contradict to eq. (10). It is therefore concluded that the CNOP $u_{0\delta}$ locates the boundary of the initial constraint.

This work by Liu[25] is a very important contribution to CNOP method, and supports the previous numerical results related to CNOPs. Besides, we note that the above proof does not need the information of gradient of the objective function. This would suggest that even if the gradient of the objective function does not exist, the above proof still holds. It indicates that CNOP could be computed without using the gradient information. Also, the property that CNOPs locate the boundary of initial constraint encourages us to reduce the constraint optimization problem related to CNOP to an unconstrained one. This can help save computation times and the computer memories.

### 1.3 Physical meanings of CNOP

CNOP has clear physical meanings[5,18,20,21]. First, if initial perturbations are expressed as initial anomalies of an anomaly model for climate, the corresponding CNOP, due to its optimality, plays the role of the optimal precursor of certain climate or weather events, which is most likely to develop into this weather or climate event. Second, if CNOP is considered to be an initial perturbation superimposed on a weather or climate event, for example, a realistic El Nino event, it acts as the initial error that has the largest effect on the prediction uncertainty. Third, in the studies of sensitivity and stability analysis, since CNOP characterizes the maximum nonlinear evolution at prediction time for the initial perturbations satisfying the given constraint, it describes the most unstable (or most sensitive) initial perturbation of the nonlinear model with the given finite time period. Finally, CNOP can also be used to estimate the upper bound of the prediction error when the initial value $U_0$ and $u_0$ are respectively considered as an initial observation and its initial observational error.

These physical meanings of CNOP have been primarily realized by applying it in ENSO predictability and the sensitivity of ocean's thermohaline circulation, which, however, are based on theoretical models and have been summarized in the paper of ref. [20]. In the following sections, we will be follow the line of physical meanings of CNOP discussed above to introduce the aforementioned ideas of CNOP in other problems of atmosphere and ocean, even coupled atmosphere-ocean system. Then the physics of CNOP could be more substantial.

## 2 CNOP as the optimal precursors for a weather or climate events

The so-called optimal precursor is referred as the initial pattern that evolves into a weather or climate event most probably. Although LSV has been used to explore the optimal precursor for ENSO events[6], it is established on that the initial perturbation is sufficiently small such that its evolution can be described by TLM. Since atmospheric and oceanic motions are generally nonlinear, the optimal precursor determined by LSV may be questionable. CNOP is directly from a nonlinear model and

has no approximation; furthermore, CNOP features the largest nonlinear evolution at prediction time. CNOP could therefore be regarded as the optimal precursor for a weather or climate event. Actually, this is one of the important physical meanings for CNOP (see section 1) and has been preliminarily realized by applying CNOP in a theoretical ENSO model[22]. Although this application used a simple model, it suggests that by exploring the evolution of the optimal precursor, CNOP can be used to investigate the dynamics of atmospheric and oceanic motions and even study the nonlinear characteristic of the development of coupled systems. In this section, we will present two examples of this kind of applications of CNOP to show the potential of CNOP in studying the evolution of weather, climate and coupled system. One is related to blocking event in atmosphere, and the other is associated with ENSO event of coupled system.

### 2.1 The initial perturbation that triggers the blocking onset

Atmospheric blocking is a typical large-scale circulation with a characteristic time scale larger than that of synoptic motions, which has long been recognized to have a profound effect on regional weather and climate[31]. LSV was used to study the involved problems such as the finite-time instability of the northern winter circulation, and the role of barotropic dynamics in the evolution of blocking, etc.[32−34]. As the aforementioned, LSV could be invalid when the nonlinearity starts to be active in the atmospheric models and therefore cannot reveal effectively the effect of nonlinearity on blocking onset. Nevertheless, Mu and Jiang[35] recently used the nonlinear technique of CNOP to explore the initial perturbation that triggers the block onset and revealed the effect of nonlinearity on the initial perturbation that triggers blocking onset. Next, we review this work to understand the effect of nonlinearity on blocking onset.

In Mu and Jiang[35], the authors used the T21L3 QG model to show that the CNOP type initial perturbation that triggers blocking onset depends on the types of objective functions. That is to say, to find the initial perturbation that yields blocking, a proper objective function related to CNOPs should be constructed. In that study, the authors constructed two kinds of objective functions to investigate the perturbations yielding blocking. One kind is based on a blocking-index form, i.e., $B=<\varphi_b,\varphi_d>/<\varphi_b,\varphi_b>$, where $\varphi_b$ is the blocking anomaly field represented by the streamfunction, $\varphi_d$ the daily streamfunction anomaly field over the climatological mean field. The angle brackets denote the Euclidean inner product on a sphere, integrated over height, $\langle x,y\rangle=\iiint xy\mathrm{d}V$, where $V$ indicates the integration over the whole atmosphere. A circulation pattern with $B\geqslant 0.5$ is defined as a blocking flow[35]. The larger $B$ is, the more pronounced the blocking flow is. Then the corresponding objective function is

$$J_N(q_{N0}^*)=\max_{\|q_0\|\leqslant\sigma}\frac{\left\langle \mathrm{E}^{-1}[M_T(Q_0+q_0)-M_T(Q_0)],\varphi_b\right\rangle}{\left\langle\varphi_b,\varphi_b\right\rangle},$$

where the streamfunction squared norm $\|q_0\|^2=[q_0, q_0]=\left\langle \mathrm{E}^{-1}q_0,\mathrm{E}^{-1}q_0\right\rangle$ is used ($\mathrm{E}^{-1}$ is the inverse operator of E, which transforms potential vorticity into streamfunction); $\sigma$ is a presumed positive constant representing an up-bound of the magnitude of the initial uncertainty; $Q_0$ is the initial potential vorticity of the reference state; $M_T$ denotes T21L3 QG model and $Q(T)=M_T(0)$. Initial perturbation $q_0$ is superimposed on the initial condition $Q_0$. Such initial perturbation $q_{N0}^*$ is called type1-CNOP, which can be transformed into the corresponding streamfunction field $\varphi_{N0}^*$. The corresponding linear counterpart, LSV, is obtained by optimizing $J_L=\left\langle\varphi_0,\mathrm{EM}^*\mathrm{E}^{-1}\varphi_b\right\rangle\Big/\left\langle\varphi_b,\varphi_b\right\rangle$, where $M^*$ is the adjoint one of the TLM for the nonlinear model $M_T$. The resultant LSV is called type1-LSV.

Another kind of objective function related to CNOP is to maximize the streamfunction squared norm under the same initial constraint condition $\|q_0\|\leqslant\sigma$, that is, $J(q_0^*)=\max_{\|q_0\|\leqslant\sigma}\left\|P(M_T(Q_0+q_0)-M_T(Q_0))\right\|$, where $P$ is an adopted projection operator for keeping consistent with the definition of type1-CNOP and $q_0^*$ is called type2-CNOP. The linear counterpart of type2-CNOP, denoted by type2-LSV, is obtained by maximizing a modified version of the objective function $J(q_0)$, which is obtained by replacing the nonlinear evolution of the perturbation by its tangent linear evolution.

In ref. [35], the case of 0000 UTC 22 January 1993 from ECMWF analysis data was chosen as initial condition of a reference run to investigate the perturbations that yield blocking. For this case, a forecast period of 6

days was adopted to calculate the CNOPs and LSVs (Figure 1). It is found that the structures of type1-CNOP and LSV both have a more global nature than type2-CNOP and LSV do. Furthermore, for the reference run, the blocking index at day 6 is $B$=0.224. The blocking index for the perturbed field of type1 CNOP is 1.732, so the transition to a blocked flow in the perturbed run is clearly visible; whereas for type1-LSV, the blocking index is 0.655, so only a weak blocking flow can be found in the perturbed run. The blocking indices for the perturbed fields after 6 days for type2-CNOP and type2-LSV are 0.319 and 0.484, respectively. It seems that neither type2-CNOP nor type2-LSV triggers a blocking onset.

Another reference run, the case of 0000 UTC 10 December 1992, was also used in ref. [35]. For the forecast period of 6 days, the obtained type 1-CNOP and LSV both have a more global nature than type 2-CNOP and LSV do. Furthermore, the projections of type2-CNOP and type2-LSV on to type1-CNOP are only 0.28 and 0.311, respectively; the similarities between them are very small, implying these two types of CNOPs and LSVs are different. As for the perturbation-triggering blocking onset, it was found that the blocking index of the reference run at day 6 is $B = -0.179$ . But the blocking indices for the perturbed fields after 6 days for type1-CNOP and type1-LSV are 1.18 and 0.479 respectively. This means that type1-LSV does not trigger the blocking onset, whereas type1-CNOP does make the large-scale zonal flow transform to a blocking flow. The blocking index for perturbed field after 6 days for type2-CNOP is 0.556, indicating a weak blocking to appear. While for type2-LSV, $B = 0.277$ , no blocking is found in the perturbed field.

From these results, it is summarized that the type1-CNOP tends to be more probably than type2-CNOP

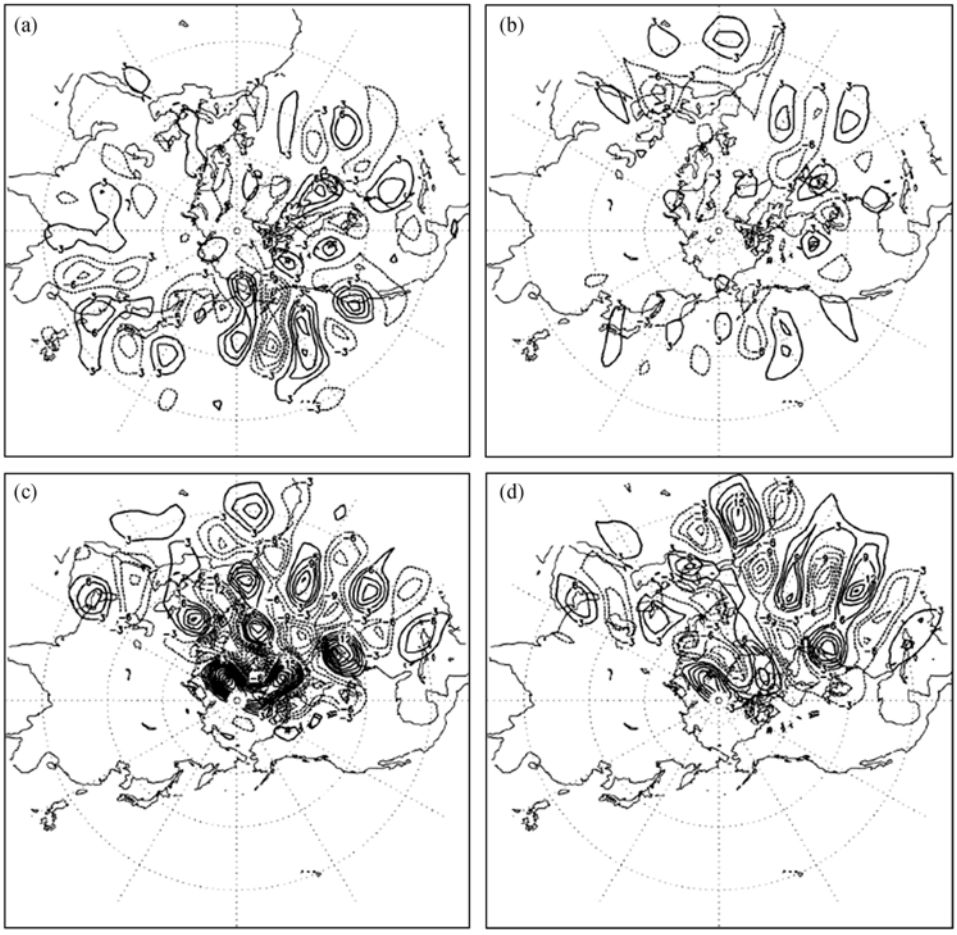


**Figure 1** Geopotential height fields with optimization time of 6 days at 500 hPa for 00 UTC 22 January 1993 of type1-CNOP (a), type1-LSV (b), type2-CNOP (c) and type2-LSV (d). In this case, CNOPs are significantly different from LSVs. Type1-CNOP and LSV have a more global nature than type2-CNOP and LSV. The patterns on them are dependent on the choosing on the objective functions. This figure is from ref. [35].

in triggering a transition to a blocking regime, which suggests that a proper objective function related to CNOP needs to be constructed in order to find the initial perturbation that most probably yields blocking onset. Although type1-CNOPs have the ability to trigger the onset of blockings, its corresponding LSVs are inclined to fail to cause a blocking onset. This difference between CNOP and LSV suggests the effect of nonlinearity on blocking onset. It is obvious that CNOP and its evolution capture the effect of nonlinearity on the initial perturbation that triggers blocking onset, while LSV is helpless. It is known that the atmospheric flow describe by T21L3 QG model is nonlinear. Therefore, we believe that CNOP is superior to LSV in finding initial perturbations that trigger blocking onset.

### 2.2 ENSO amplitude asymmetry

Section 2.1 comments on the application of CNOP in finding the initial perturbation that triggers blocking onset, which, in fact, applies CNOP to reveal the optimal precursor for blocking onset. This application of CNOP is related to atmospheric motion. In the following, the physics of CNOP as optimal precursor is also involved into coupled atmosphere-ocean system, that is, the problem of ENSO amplitude asymmetry.

ENSO amplitude asymmetry is an important problem of ENSO studies. The ENSO asymmetry is referred to the phenomenon that the amplitude of the observed El Nino is larger than that of La Nina. This is a distinct feature of ENSO[22,36,37]. Furthermore, there is evidence that ENSO amplitude asymmetry has become pronounced since the climate shift around the year 1976, from a relatively stable to an unstable oscillating system[38,39]. We have known that the linear dynamics of ENSO provided essential insights into the mechanisms responsible for the periodicity of ENSO[40,41], but it cannot explain what governs its amplitude. Furthermore, Duan et al.[22], An and Jin[37], and Rodgers et al.[42] used respectively a nonlinear ENSO system to study the ENSO amplitude asymmetry; they demonstrated coherently that ENSO amplitude asymmetry is a typical nonlinear property of coupled ocean-atmosphere system. In other words, ENSO amplitude may be controlled by a nonlinear system. Consequently, the nonlinear chaotic theory of ENSO could be more reasonable than the linear theory. In an ENSO model, there exist several nonlinear physical processes. Then which process plays the essential role in ENSO amplitude asymmetry? The work of Duan et al.[43] on CNOP's applications to ENSO study gives an answer to this question.

Duan and Mu[39] have demonstrated that nonlinearity induces the ENSO asymmetry. The stronger ENSO events are, the stronger the nonlinearities are, and the more significant ENSO asymmetry is. It is obvious that ENSO asymmetry is related to strong ENSO events. CNOPs, rather than LSVs, are the optimal precursors that evolve into ENSO events[22]. The ENSO events caused by the CNOP-type precursors are the strongest ones for a given initial constraint. It is therefore reasonable that CNOP is more applicable than LSV in revealing the ENSO amplitude asymmetry with CNOP as optimal precursors for ENSO events.

For this reason, Duan et al.[43] directly used the approach of CNOP to investigate the roles of different types of nonlinearities in ENSO asymmetry and showed the decisive role of nonlinear temperature advection (NTA). They adopted both the theoretical model developed by Wang and Fang[44] and the intermediate Zebiak-Cane model[45]. By investigating the El Nino and La Nina events caused by CNOP-type precursors, they demonstrated that the El Nino event caused by the CNOP in the WF96 model is drastically stronger than the La Nina event caused by the local CNOP (Figure 2). The stronger the El Nino event is, the more significant the ENSO asymmetry is Figure 3. It was further shown that the evolutions of CNOP and local CNOP in the TLM also evolve respectively into an El Nino event and a La Nina event, but they tend to be symmetric in amplitude. Furthermore, the amplitude of the El Nino in the TLM is considerably smaller than that of the El Nino in the WF96 model, while the La Nina events in the WF96 model and its TLM remain similar. This difference between nonlinear and linear cases shows that nonlinearity plays an important role in ENSO asymmetry. The nonlinearity enhances El Nino and affects trivially La Nina, causing ENSO amplitude asymmetry. Similar results are obtained in the Zebiak-Cane model. By analyzing the roles of different nonlinearity terms in the Zebiak-Cane model, Duan et al.[43] clearly identified the origin of ENSO asymmetry. In fact, in the Zebiak-Cane model, there are three kinds of nonlinearities: nonlinear temperature advection, subsurface temperature parameterization, and the wind stress term. Among the three nonlinearities, the effect of the nonlinearity of the subsurface temperature parameterization on ENSO asymmetry can be offset by that of the wind stress anomaly,

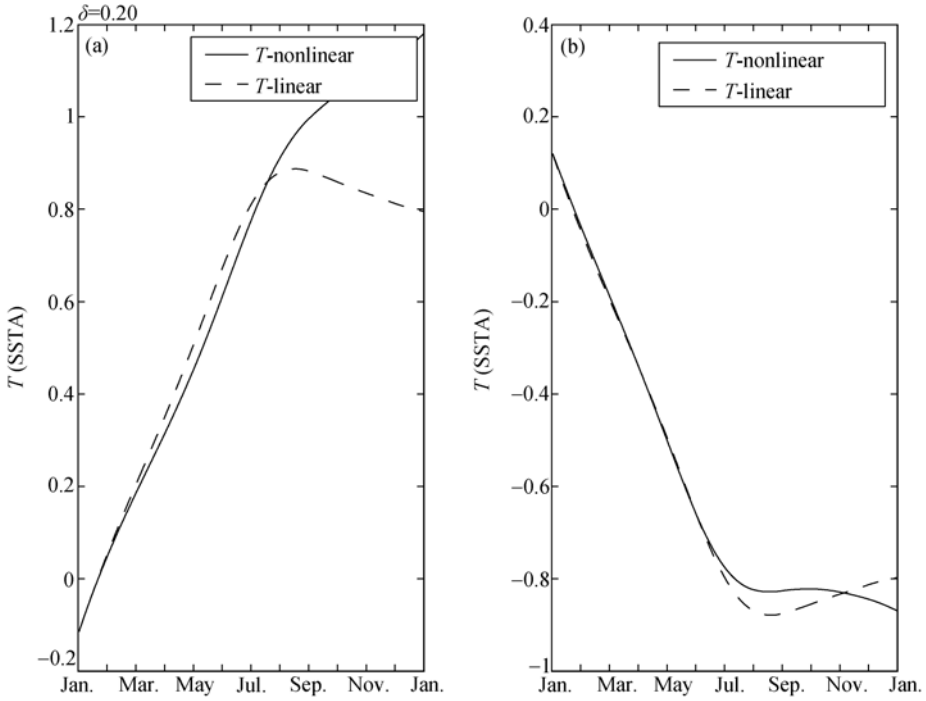


**Figure 2** Nonlinear and linear evolutions of CNOPs. (a) The nonlinear and linear evolutions of CNOP (of WF96 model). They correspond to an El Nino event, respectively. The El Nino with nonlinear evolution is stronger than that with linear evolution. Nonlinearity enhances El Nino. (b) The nonlinear and linear evolutions of local CNOP. They correspond to a La Nina event, respectively. These two La Nina events have similar intensities. Nonlinearity has trivial effect on La Nina amplitudes. The El Nino with nonlinear evolution is significantly stronger than the La Nina with nonlinear evolution, but the El Nino and La Nina events with linear evolutions have almost the same amplitudes. The ENSO events in WF96 model are asymmetric, but those in the linearized model are almost symmetric. This figure is from ref. [43].

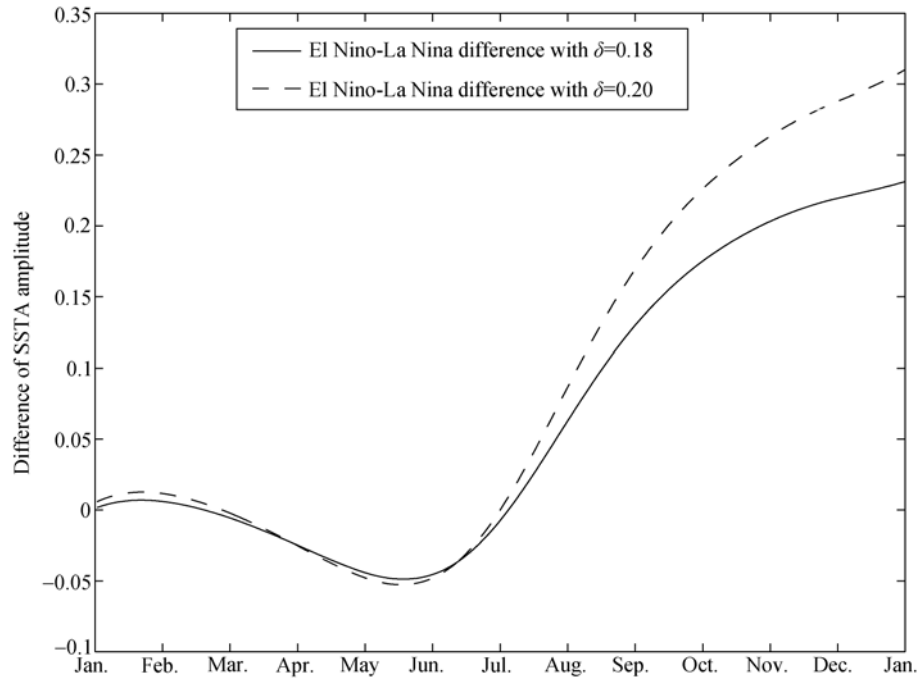


**Figure 3** Solid line (dashed line) represents the difference of amplitudes between El Nino and La Nina caused by CNOPs with magnitude 0.18 (0.20) in terms of norm. The larger the CNOPs are, the stronger the ENSO events are, and the more significant the ENSO asymmetry is (which is indicated by the large amplitude difference). This figure is from ref. [43].

which leaves the nonlinearity related to the nonlinear temperature advection to play the decisive role in ENSO asymmetry (Figure 4). These results of the Zebiak-Cane model support those of the WF96 model. That is, the nonlinear temperature advection considerably enhances El Nino and trivially affects La Nina amplitude.

The work of Duan et al.[43] analyzed the roles of different nonlinearities in ENSO asymmetry and illustrated a clear route to ENSO asymmetry by CNOP approach. The strong ENSO asymmetry with strong nonlinearity of strong ENSO events indicates why the ENSO asymmetry becomes strong after the 1970s. That is to say, the decadal change of ENSO asymmetry may be due to the change of nonlinearity. If such, CNOP approach could be extended to study the decadal variability of ENSO[39]. It is therefore expected that scientists attempt to apply it in the studies of decadal variability of ENSO or others.

## 3 CNOP as the initial error that has the largest negative effect on predictions

As mentioned earlier, when initial perturbations are superimposed on a weather or climate events, CNOP acts as the initial error that has the largest negative effect on predictions. Although LSV was used to estimate the initial error that has the largest effect on prediction[6,13], it could be invalid in a nonlinear model. Then CNOP has been used to study the initial error that causes the largest prediction error[9,10,18]. Especially, CNOP has been used to explore the initial error that causes a significant SPB phenomenon[9,10] in a theoretical ENSO model and revealed the effect of nonlinearity on SPB. Recently, CNOP has further been applied to investigating the SPB in a realistic model[10] and obtained the spatial patterns of initial error that cause a significant SPB. The SPB is referred to a phenomenon that most ENSO prediction models often experience an apparent drop in prediction skill across April and May[46]. A significant SPB can be measured from two aspects: the large prediction error and the obvious seasonality of error growth. CNOP type error causes the largest prediction error and has notable season-dependent evolution in ENSO models, then inducing significant SPB for ENSO. In ref. [10], the authors utilized the physics of CNOP as the initial error that has the largest effect on prediction to investigate SPB. In this section, we focus on reviewing this work.

The problem of SPB for ENSO is an important aspect of ENSO predictability studies. Many works have investigated this phenomenon (see the review of ref. [47]). In particular, Chen et al.[48] reported that by using the initial field produced by a data assimilation approach, the SPB in the ZC model is not as severe as that in persistence or in most other forecast models, which indicates the importance of the accuracy of initial fields in ENSO predictability. To investigate the initial error patterns that cause a significant SPB for ENSO event, Moore and

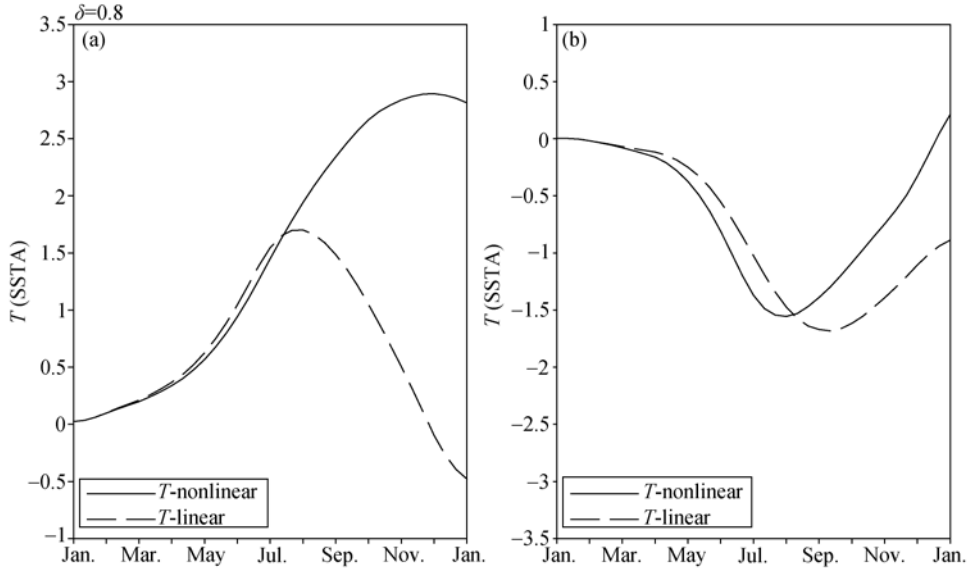


**Figure 4** SSTA components of the evolutions of CNOP (local CNOP) for constraint bound as 0.8 in the ZC model (solid line) and PL-ZC model (dashed line; the model that only the nonlinear temperature advection term is linearized). (a) For El Nino events caused by CNOP; (b) for La Nina events caused by local CNOP. The El Nino and La Nina in ZC model are asymmetric, but those in PL-ZC model are symmetric. Nonlinear temperature advection plays the decisive role in ENSO amplitude asymmetry. This figure is from ref. [43].

Kleeman[6], Samelson and Tziperman[7], etc. used the LSV method to address this question. It has been known that LSV is based on a TLM and cannot explore the effect of finite amplitude initial errors on prediction results. Nevertheless, it is delectable that the work of ref. [10] could remedy the limitation of LSV in studying SPB.

Mu et al.[10] used CNOP approach, rather than LSV, to investigate the SPB problem for ENSO events in the ZC model. Figure 5 shows four CNOP-type errors superimposed on an El Nino event with the start months January, April, October, and November, denoted by $R^1_{\text{Jan.}}$, $R^1_{\text{Apr.}}$, $R^1_{\text{Jul.}}$, and $R^1_{\text{Oct.}}$, respectively. According to Mu et al.[10], these CNOP-type errors yield a significant SPB phenomenon. To facilitate the discussion, we cite in Table 1 the seasonal growth rates of CNOP-type errors obtained by ref. [10]. From the data shown in Table 1, the largest growth of the CNOP-type errors occurs in AMJ (that is, April-May-June, which is through boreal spring and the beginning of summer). Furthermore, these CNOP-type errors cause the severest NINO3 SSTA prediction error (denoted by "$E_{\text{Nino-3}}$" in Table 1) due to their optimality. It is conceivable that due to the spring largest error growth, the prediction skill of El Nino will decrease dramatically through spring and yields the SPB phenomenon. On the other hand, Mu et al.[10] found that some other kinds of initial errors (including LSVs) (Figure 6), whose patterns are different from those of CNOPs, either show less prominent season-dependent evolutions or have a trivial effect on the forecast results, and consequently do not yield significant SPB (see Table 2), although the magnitudes of such initial errors are the same as those of CNOPs in terms of

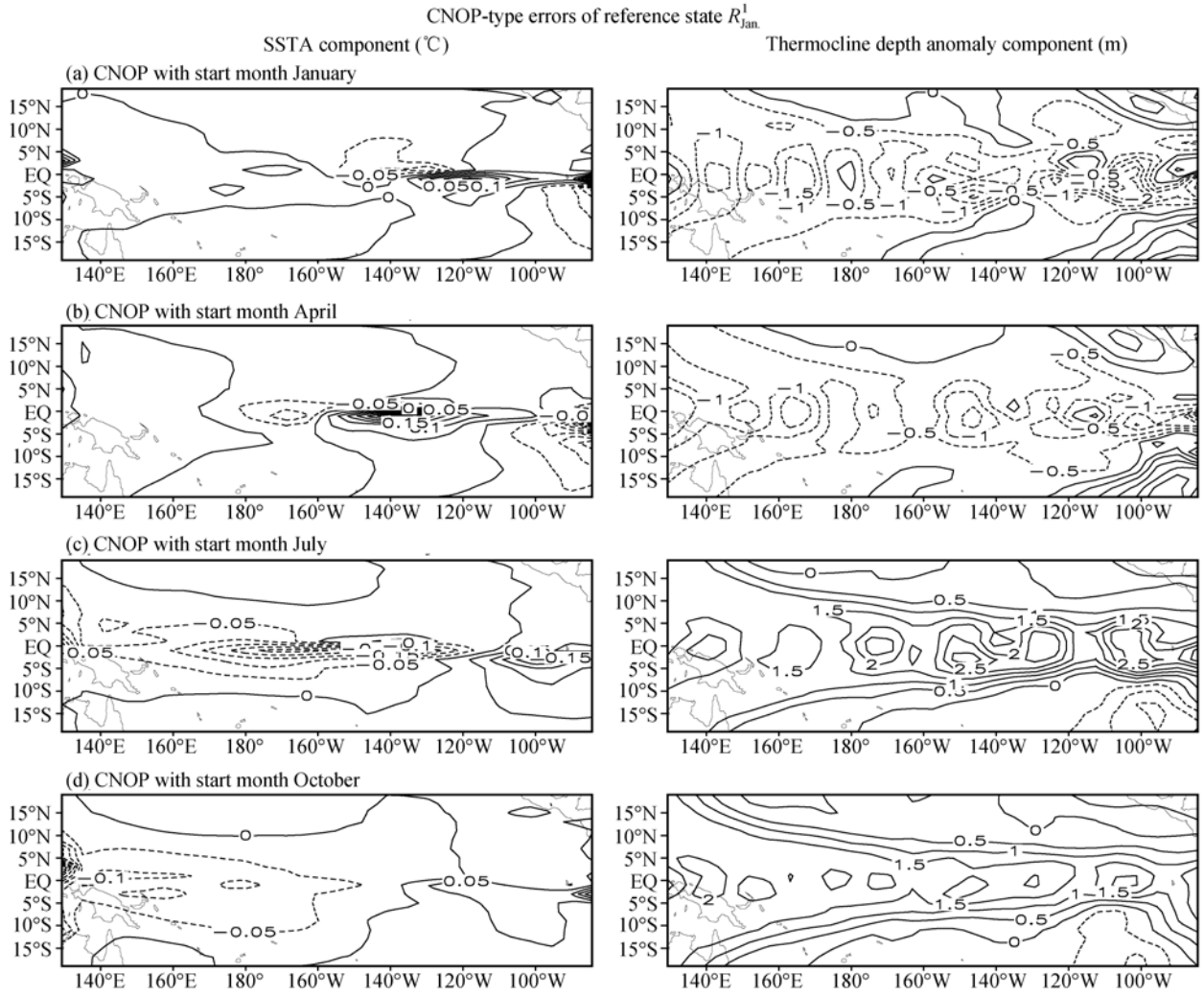


**Figure 5** The patterns of CNOP-type error for a given El Nino event in the ZC model. SSTA (left) and thermocline depth anomaly components (right) for the start month being January (a), April (b), July (c), and October (d). This figure is from ref. [10].

**Table 1** Growth rates of CNOP-type error evolutions for start month October (from ref. [10])

| Reference states | OND | JFM | AMJ | JAS | $E_{\text{Nino-3}}$ |
|---|---|---|---|---|---|
| $R^1_{\text{Jan.}}$ | 1.3507 | 2.1358 | **6.3777** | 1.1392 | 1.6711 |
| $R^1_{\text{Apr.}}$ | 1.2216 | 1.6740 | **5.0808** | 3.5340 | 2.0953 |
| $R^1_{\text{Jul.}}$ | 2.1358 | 3.6559 | **7.7281** | 1.7341 | –2.4585 |
| $R^1_{\text{Oct.}}$ | 1.9107 | 3.5522 | **7.6553** | 3.1489 | –2.7356 |

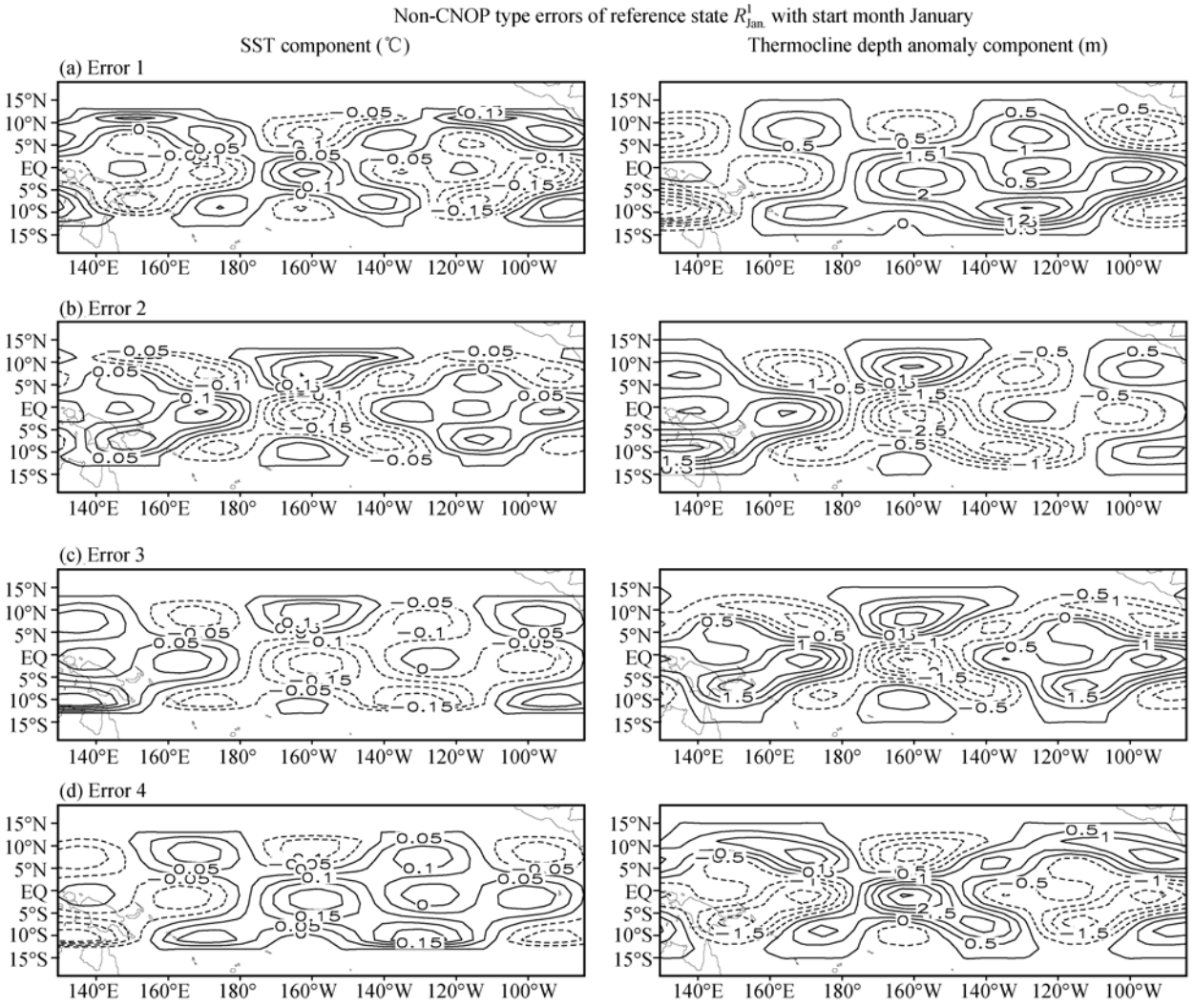


**Figure 6** Four representatives of Non-CNOP type errors for the given El Nino event, where the start month of prediction is January. SSTA (left) and thermocline depth anomaly components (right). This figure is from ref. [10].

**Table 2** Growth rates of Non-CNOP type error evolutions for start month January for a given El Nino (from ref. [10])

| Error type | JFM | AMJ | JAS | OND | $E_{\text{Nino-3}}$ |
|---|---|---|---|---|---|
| CNOP | 0.8481 | **4.1740** | **8.8463** | 0.4555 | –2.3865 |
| Non-CNOP 1 | –0.4929 | 0.2541 | 0.1709 | –0.2311 | –0.0757 |
| Non-CNOP 2 | –0.5411 | 0.1659 | 0.1831 | –0.1795 | 0.0351 |
| Non-CNOP 3 | –0.4126 | –0.0708 | 0.3766 | 0.0625 | 0.0853 |
| Non-CNOP 4 | –0.3887 | –0.1195 | 0.3523 | 0.1517 | –0.1252 |

the chosen norm.

From these results of ref. [10], it is suggested that the SPB for El Nino events could be closely related to the particular pattern of initial error. Different error patterns

cause different amplitudes of spring error growth related to season-dependent evolutions. Due to the significant season-dependent evolution of CNOP-type errors and its resultant largest prediction errors, it is reasonable to consider CNOP-type errors as one of candidate errors that cause a significant SPB.

SPB is one of the unresolved problems for ENSO. The above study is on seasonal dependence of error growth for El Nino events under the assumption of perfect model. That is to say, the above study involved the first kind of predictability experiments of theoretical El Nino events, which indicates that if a data assimilation approach possess the function of filtering the CNOP-type or (and) other similar errors, it is hopeful to improve the prediction skill of ENSO. To serve this goal, we suggest that the future works should address whether the results obtained in this paper is model dependent. Besides, we note that CNOP-type error has a localized region and may capture the sensitive area of ENSO prediction. If so, some hindcast experiments should be performed to examine the effectiveness of the sensitive area determined by CNOP. It is then hopeful that CNOP is gradually applied in realistic ENSO predictions and attempt to improve ENSO forecast skill.

## 4 CNOP as the most unstable (or most sensitive) mode in stability and sensitivity analysis

In the previous sections, we have reviewed the applications of CNOP in the dynamics studies of atmosphere (for example, blocking event) and coupled ocean- atmosphere system (for example, ENSO asymmetry), also in the predictability studies of coupled ENSO system (for example, the SPB for ENSO events). In the studies of atmosphere dynamics, CNOPs can act as the initial perturbation that yields a certain weather event most probably (for example, a blocking onset), and in coupled ocean-atmosphere system, CNOP can play the optimal precursor for a climate event (for example, ENSO event). In predictability studies, CNOPs stands for a kind of initial error that is superimposed on a weather and climate event and has the largest effect on the prediction results. From the definition of CNOP, we note that CNOP is an initial perturbation on a reference state, of which the amplification reflects the extent of the stability of the reference state. For CNOP itself, since it possesses the largest nonlinear evolution at prediction time, it represents the most unstable (sensitive) mode. Along this thinking, CNOP can be used to sensitivity analysis (and stability analysis) of atmosphere, ocean, and coupled atmosphere-ocean, etc. In fact, this physical meaning of CNOP has been used to estimate the sensitivity of ocean's thermohaline circulation in a theoretical model[23,24]. Recently, it has further extended to the stability studies of atmospheric baroclinic unstable flows and ocean's double-gyre flow, and the sensitivity analysis of ecosystem. Furthermore, in the sensitivity analysis of ecosystem, the problem of the transition between equilibrium states is involved. This suggests that CNOP is also potential for exploring the transition between equilibrium states. To make the authors have a clear diagram about CNOP's application to the sensitivity analysis, we introduce in the following the recent applications of CNOP in stability and sensitivity analysis.

### 4.1 Nonlinear behavior of baroclinic unstable flows

The properties of baroclinic instability have been extensively studied in linear approximation since the pioneering work of Charney[49] and Eady[50]. Two techniques are traditionally used to study the linear instability problem. The first one uses the normal mode approach. Such a method presents the disadvantage that it fails to capture localized disturbances that can have a rapid growth over a limited period in time[51,52]. A second approach consists of identifying "optimal perturbations" (i.e. LSVs) that maximize the growth rate over a given time interval[42]. This idea has been applied in predictability studies, and it has been shown that SVs capture the essential ingredients of growth of extratropical synoptic systems[53]. However, their main disadvantage is that they are based on a linearized equation. Under the linear assumption, positive and negative perturbations have the same growth rate although they can evolve rather differently under nonlinear dynamics. In addition, the growth of the SVs in the nonlinear system can be greatly reduced compared to the growth in the linear case. It is therefore questionable whether the optimality of SVs is still valid for the original nonlinear problem.

Considering that the linearity of SVs does not take into account some mechanisms presented during the nonlinear development (such as wave-mean flow interactions), Riviere et al.[26] applied a CNOP-like approach, a modified version of nonlinear singular vector (NLSV) approach developed by Mu[17], in a two-layer quasi-geostrophic model to investigate the effect of nonlin-

earities on the behavior of baroclinic unstable flows. In that study, the authors defined the objective function related to the so-called NLSV with perturbation growth rate, and confined the initial perturbations on the boundary of a constraint. That is,

$$J(u_{0\delta}) = \max_{\|u_0\|=\sigma} \frac{\| M_\tau(U_0+u_0) - M_\tau(U_0) \|}{\| u_0 \|}. \quad (11)$$

Since the constraint is $\|u_0\|=\sigma$ ($\sigma$ is a constant), the optimal perturbation $u_{0\delta}$ in eq. (11) is equivalent to that in eq. (12) although they have different values of the objective functions:

$$J_1(u_{0\delta}) = \max_{\|u_0\|=\sigma} \| M_\tau(U_0+u_0) - M_\tau(U_0) \|. \quad (12)$$

Mu et al.[18] pointed out that the initial perturbations related to CNOP can be constrained by inequality, equality or other kinds of functional set or some physical law. Thus, the optimal perturbations obtained by eq. (12) are also a kind of CNOP. That is to say, NLSVs in ref. [26] are also CNOPs. Therefore, we use the terminology of CNOP to describe the results of ref. [26].

Riviere et al.[26] demonstrated that for small energies, the CNOP and SV have very similar spatial structures (compare Figures 7(b) and 8(a)); when the initial energy is increased, the structures of the CNOP and SV at initial time begin to differ (compare Figures 7(b) and 8(b)—(d)); an asymmetry in the initial location of positive and negative PV anomalies can be observed: positive upper-layer and negative lower-layer PV anomalies tend to be on the poleward side of the jet, while opposite anomalies are on the equatorward side of the jet. This

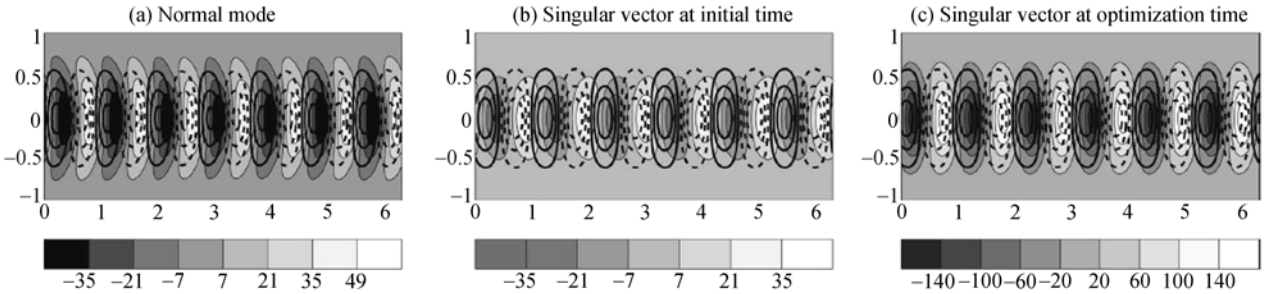


**Figure 7** Snapshot of normal mode with an initial energy $E_0$ =0.5 (a), the leading SV at initial time (b) and at final time (in the tangent linear model) (c). The filled contours represent the upper-layer potential vorticity (PV) and the solid and dashed contours represent the lower-layer PV (solid for positive values and dashed for negative values). Negative and positive values have the same contour intervals. This figure is from ref. [26].

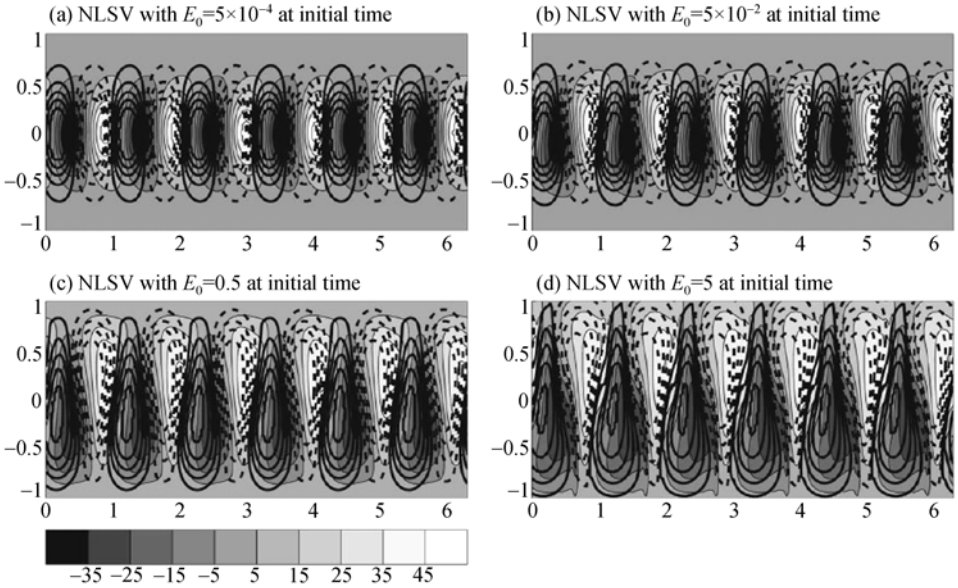


**Figure 8** PV of the NLSV (total energy norm) at initial time for different initial energies: $E_0$= 5×10$^{-4}$ (a), 5×10$^{-2}$ (b), 0.5 (c), 5 (d). Contours have the same definition as in Figure 1. This figure is from ref. [26].

asymmetry cannot be observed from the SV pattern (see Figure 7(b)). Also, with the increasing initial energy, an increase in the latitudinal extension of the patterns is shown in CNOPs (see Figure 8(a)—(d)), of which this phenomenon cannot be demonstrated by LSV method.

Another important difference between the SV and the CNOP at initial time is that the CNOP possesses a zonal-mean shear in the same direction as the basic jet, but with retrograde jets on both sides (compare Figure 9(b) and (c)). This reinforces the basic jet so that the final mean shear of the CNOP is smaller than in the SV case. This indicates that the zonal-shear in CNOP pattern increases the initial extraction of energy from the total shear (basic plus zonal-mean flows) and opposes wave-mean flow interactions that decrease the shear through the nonlinear evolution. This kind of spatial shape of the CNOPs (especially their meridional elongation as in Figure 8) allows them to limit wave-wave interactions. These wave-wave interactions are responsible for the formation of vortices and for a smaller extraction of energy from the basic flow. Therefore, Riviere et al.[26] implies that CNOPs can modify their shape in order to evolve quasi-linearly to preserve a large nonlinear growth.

It is obvious that CNOPs computed by ref. [26] show effect of nonlinearities on the baroclinic unstable flows, of which an important finding is that CNOP patterns present the initial zonal-mean shear structure, which, however, cannot be shown by LSV pattern. SVs have limitations in exploring the optimal sensitivity of baroclinic flows. However, CNOP can remedy it. This contribution adds confidence to the potential of CNOP for revealing the nonlinearity in stability studies of atmosphere dynamical behavior. Next, we turn to introduce the application of CNOP in sensitivity analysis of ocean's circulation.

### 4.2 Sensitivity of ocean's double-gyre flow

One of recent applications of CNOP to ocean's circulations is on sensitivity analysis of double-gyre ocean circulation. The so-called quasi-geostrophic double-gyre flow has been recognized as one of the characteristic problems to study the nonlinear dynamics of the wind-driven ocean circulation[54,55]. The linear problems, neglecting inertia, are the basis for the Sverdrup-Stommel-Munk theory of the wind-driven ocean circulation. The generalized stability theory has been used to explore such kinds of problems[56]. However, in this case, it is usually assumed that the initial perturbation is so small that its evolution can be described by a linearized system (the tangent linear model) and optimal growth is determined through the largest singular value (the growth rate of the first LSV) of the forward propagator of the linearized system. This may limit the usefulness of LSV in nonlinear field related to ocean's circulations.

To address the effect of nonlinearity on the finite amplitude stability of the double-gyre flow, Terwisscha van Scheltinga[27] used an implicit 4D-Var methodology to compute the CNOPs of the double-gyre ocean circulation described by the barotropic quasi-geostrophic model. They showed that under symmetric wind-stress forcing, in the asymptotically stable regime of the anti-symmetric state, the patterns of the CNOPs at short optimization time scales are very similar those found in energy stability studies[56] (comparing Figure 10(a) with Figure 7(b) of Dijkstra[55]), which indicates that in the conditional stability regime the pattern of the energy stability analysis is relevant for short times. When the CNOP is computed for larger time periods, although the pattern of CNOPs keeps the same symmetric structure, the pattern extends locally in size (see Figure 10(b)—(d)).

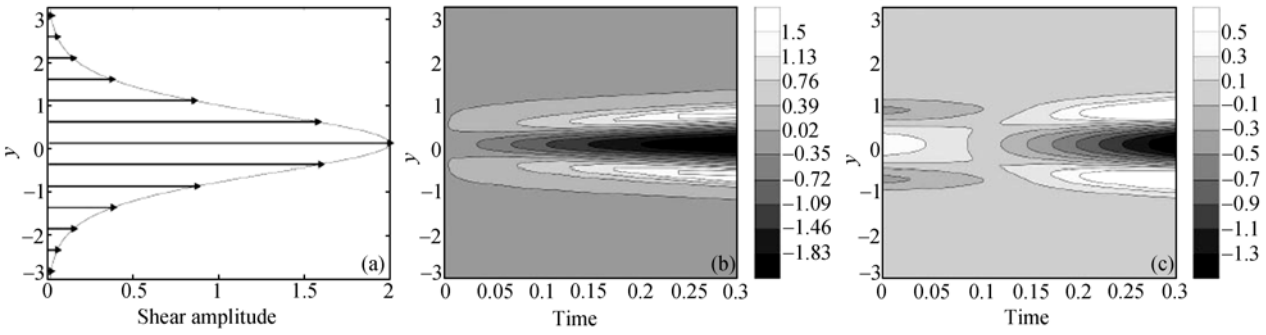


**Figure 9** Zonal-mean shear of the basic jet. Zonal-mean shear as a function of time (abscissa) and $y$ (ordinate), for the SV in the nonlinear model (b) and NLSV (c). For these cases $E_0$=0.5. CNOP possesses a zonal-mean shear in the same direction as the basic jet, but LSV does not. This figure is from ref. [26].

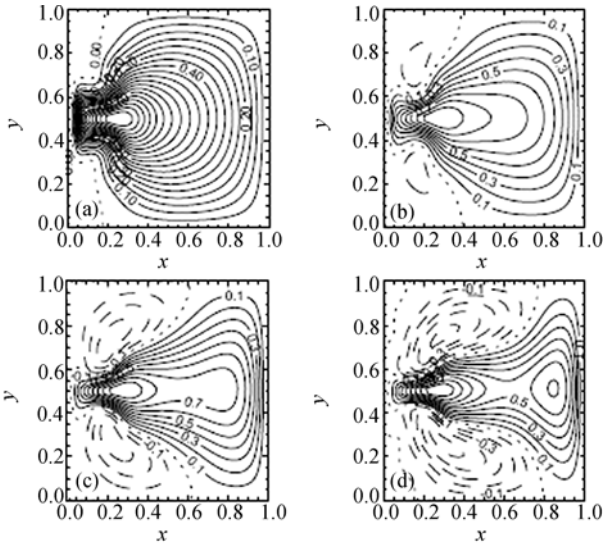


**Figure 10** Patterns of the barotropic streamfunction for the CNOPs of a steady state for the optimization time period te=7 days (a), te=14 (b), te=21 days (c), and te=28 days (d). For the short time period 7 days, the CNOP pattern is very similar to that obtained by energy (linear) stability analysis; with the increasing of the optimization time periods, the CNOP patterns become more and more local regions, indicating that the nonlinear effect is more and more considerable. This figure is from ref. [27].

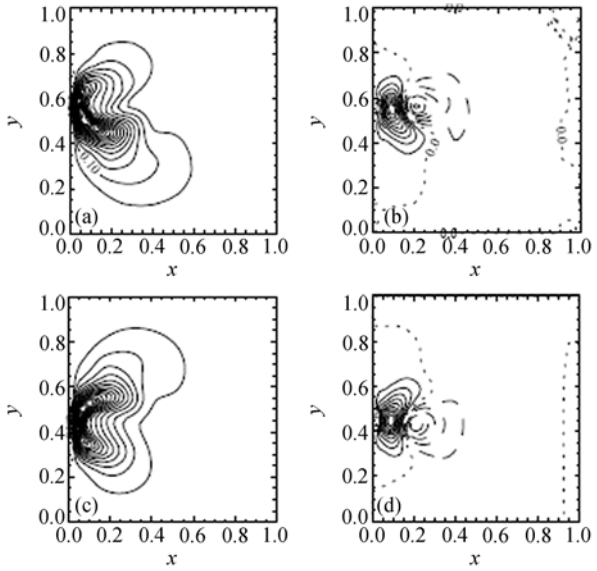


**Figure 11** Cases for symmetric wind stress. (a) CNOP for the jet-down steady state; (b) the deviation of the CNOP-evolution flow from the jet-down steady state after 7 days; (c) CNOP for the jet-up steady state; (d) the deviation of the CNOP-evolution flow from the jet-up steady state after 7 days. This figure is from ref. [27].

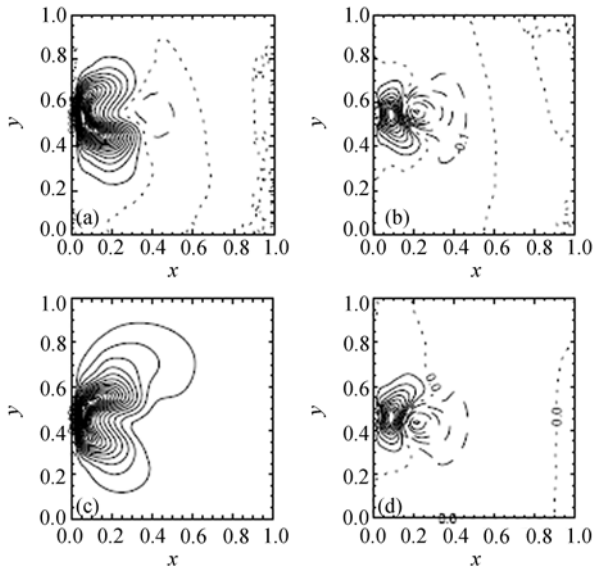


**Figure 12** Cases for asymmetric wind stress. (a) CNOP for the jet-down steady state; (b) the deviation of the CNOP-evolution flow from the jet-down steady state after 7 days; (c) CNOP for the jet-up steady state, and (d) the deviation of the CNOP-evolution flow from the jet-up steady state after 7 days. This figure is from ref. [27].

In the asymmetric branches for which two asymmetric steady solutions (jet-up state and the jet-down state) are linearly stable, the CNOP patterns of these two states for optimization time period 7 days are no longer symmetric because of the asymmetry of the background state and it already quite localized near the western boundary current region (see Figure 11(a) and (c)). When the two steady states are perturbed with these CNOPs, the deviation from the steady state after 7 days (Figure 11(b) and (d)) shows a bipolar pattern resembling one phase of a Rossby basin mode. This is an oscillatory normal mode to which the steady state becomes unstable. Considering that the perturbations obtained by linear theory may not be the optimal ones and do not have the largest evolution, it is conceivable that CNOPs for larger times are the initial perturbations that most probably induce a response to the direction of the normal mode.

For the slightly asymmetric wind stress, an imperfect pitchfork occurs in the model. CNOP patterns slightly differ between the two cases of symmetric and asymmetric wind stress. The CNOP pattern for the jet-down state seems less deformed from the symmetric case (compare Figure 12(a) with Figure 11(a)). The CNOP pattern for the jet-up solution on the contrary has deformed substantially (compare Figure 12(c) with Figure 11(c)). The evolution of both CNOPs eventually leads to anomalies which have a pattern resembling a Rossby-basin mode, just as in the symmetric case, inducing a response to the direction of the normal mode.

It is obvious from the above results that for a stable steady state, a CNOP superimposed on it tends to yield an unstable behavior. Since energy linear stability analysis is related to short time scales and cannot consider the

evolutions of finite amplitude perturbations, CNOP, due to its resultant largest nonlinear evolution, is the initial perturbation that induces an unstable behavior most probably.

The above work applied CNOP to the sensitivity analysis of ocean's circulation. It is suggested that the CNOPs of a steady state determine the dominant time-dependent nonlinear behavior of finite amplitude perturbations. On one hand, such behavior bridges the gap between the behavior below the energy stability boundary (monotonic decay of all perturbations) and above the linear stability boundary (exponential growth of infinitesimally small perturbations). On the other hand, when compared to non-normal modes, the CNOP displays how much nonlinearity affects the evolution of finite amplitude perturbations[27]. Practically, this idea on CNOP can not only be used to estimate the sensitivity of the ocean's circulation, but also the sensitivity of other systems, for example, ecosystem.

### 4.3 Applications of CNOP in sensitivity analysis of ecosystem

CNOP has been applied in sensitivity and stability analysis of baroclinic unstable flow and ocean's circulations[23,24,57]. Recently, Mu and Wang[58] has further extended the application of CNOP to the sensitivity analysis of grassland ecosystem, in attempt to reveal the effect of nonlinearity on the transition between grassland and desert states.

In the studies of sensitivity analysis of ecosystem, the problem of the transition between different ecosystem equilibriums is very important, which is to investigate the coexistence of grassland and desert and whether and how human activities and natural factors induce the transitions between them. Zeng et al.[59, 60] and Zeng and Zeng[61] established simple prognostic model with three-variable grassland ecosystem. This model is mathematically simple, possesses essential processes, and has shown a potential applicability in theoretical research and a better understanding of the mechanism of the ecosystem. Using linear stability analysis approach, Zeng et al.[60] found that the three-variable model has multiple equilibrium states with certain parameter values and there exist two bifurcation points. Although LSV can be used to investigate the stability analysis of ecosystem, it is not the optimal perturbation of a nonlinear system and cannot describe the most unstable (most sensitive) mode. Furthermore, we note that the model of Zeng et al.[60] is a nonlinear ecosystem. If one uses this model to study the effects of human activities and natural variations on the ecosystem, one should consider the nonlinear instability and sensitivity in this model. Then what is the effect of nonlinearity on the sensitivity of grassland ecosystem? This question motivated the work of Mu and Wang[58].

Mu and Wang[58] used this three-variable theoretical model to attack the nonlinear instability and sensitivity of ecosystem. The results showed that the moisture index $\mu$ plays an essential role in the grassland ecosystem illustrated by the adopted model. When $\mu$ is less than the bifurcation point $\mu_1$, desert equilibrium state (DES) is nonlinearly stable even for the large initial finite-amplitude perturbations (Figure 13(a)—(c)), which implies the ecosystem is droughty and nonlinearly stable. It is impossible to change the desert state into a grassland state just by planting grass or irrigating. For the moisture index $\mu$ being larger than the bifurcation point $\mu_2$, grassland equilibrium state (GES) is conditionally nonlinearly stable. That is, there exists a threshold value of initial perturbation (denoted by $\delta$), $\delta$=1.04795, which just is the mass density of living grass ($\overline{x}$) in the grassland equilibrium state; when the magnitude of an initial perturbation $\delta$ is smaller than $\overline{x}$, there is no initial perturbation to cause a transition from it to DES; but for the case of $\delta \geqslant \overline{x}$, if a destructive action is made such that the value of the living grass component of the initial perturbation is null, the ecosystem will evolve to DES. This case suggests that it is still important to keep the balance for the ecosystem even if the soil is washy and the natural condition is feasible. When $\mu$ is between $\mu_1$ and $\mu_2$, the grassland ecosystem is fragile, GES (DES) is linearly stable but nonlinearly unstable, meaning that a large enough initial finite-amplitude perturbation can induce a transition from GES (DES) to DES (GES). It is suggested that the management of human activities is important when moisture index $\mu$ is in ($\mu_1$, $\mu_2$).

To explore the nonlinear feature of the ecosystem, Mu and Wang[58] also calculated the LSVs of GESs and DESs. Comparisons between their nonlinear evolutions demonstrated that for the same magnitude of CNOP and LSV, CNOPs tend to be more likely to yield a transition than LSVs do (Figure 14).

The above studies applied CNOP to estimate the sensitivity of ecosystem. Especially, CNOP was used to tackle the problem of the transition between equilibrium

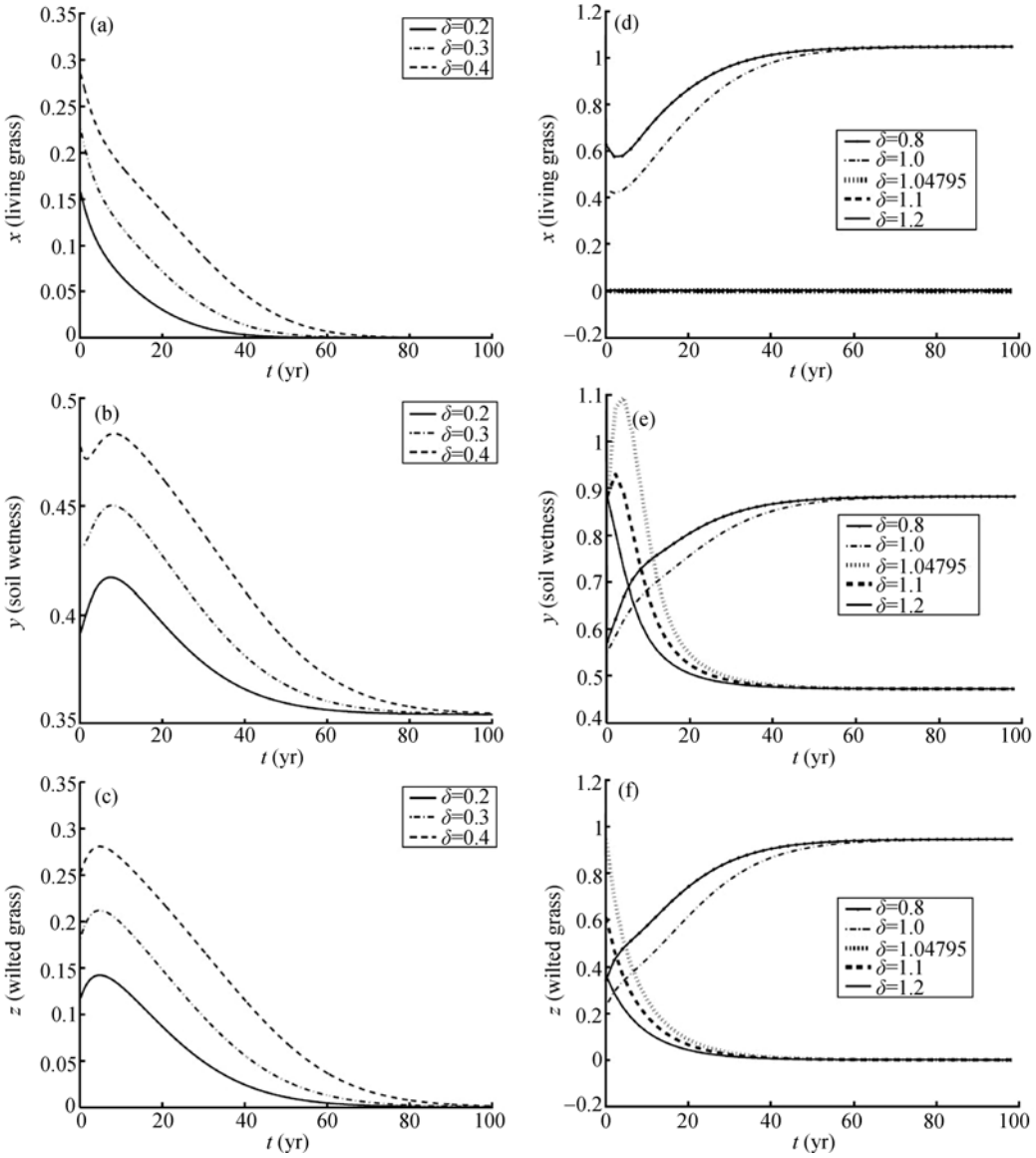


**Figure 13** The 100-year nonlinear evolutions of the ecosystem, left (right) column: CNOPs plus a DES equilibrium state (a GES equilibrium state) as initial conditions, where $\mu$=0.30 ($\mu$=0.38). $\mu_1$=0.3104 and $\mu_2$=0.3745 are two bifurcation pints. When $\mu>\mu_1$, DES is nonlinearly stable even for large amplitude initial perturbations, implying the ecosystem is droughty and nonlinearly stable. When $\mu>\mu_2$, GES is conditionally nonlinearly stable. That is, when the initial perturbation is larger than 1.04795 in terms of the chosen norm, i.e., $\delta$> 1.04795, GES is nonlinear unstable. This figure is from ref. [58].

states. The transition between equilibrium states is a typical nonlinear property[62,63]. A finite amplitude initial perturbation superimposed on an equilibrium state will cause the state developing to another equilibrium state. CNOP's application in this field could help address the mechanism of the transition between equilibrium states.

## 5 Applications of CNOP in the studies of ensemble forecasting and target observation

The aforementioned applications of CNOP involve stability and sensitivity analysis, and predictability studies, which respectively make use of the physical meanings of CNOP with it acting as optimal precursors, the most unstable mode, and the initial errors that have the largest effect on prediction results. These applications include the studies of not only atmospheric dynamics, but also oceanic dynamics and coupled system dynamics. Furthermore, CNOP is also used to the predictability studies of coupled ENSO system.

It has been known that LSV method can be used to generate the initial perturbation field of ensemble forecast[64,65] and to identify the sensitive area of target ob-

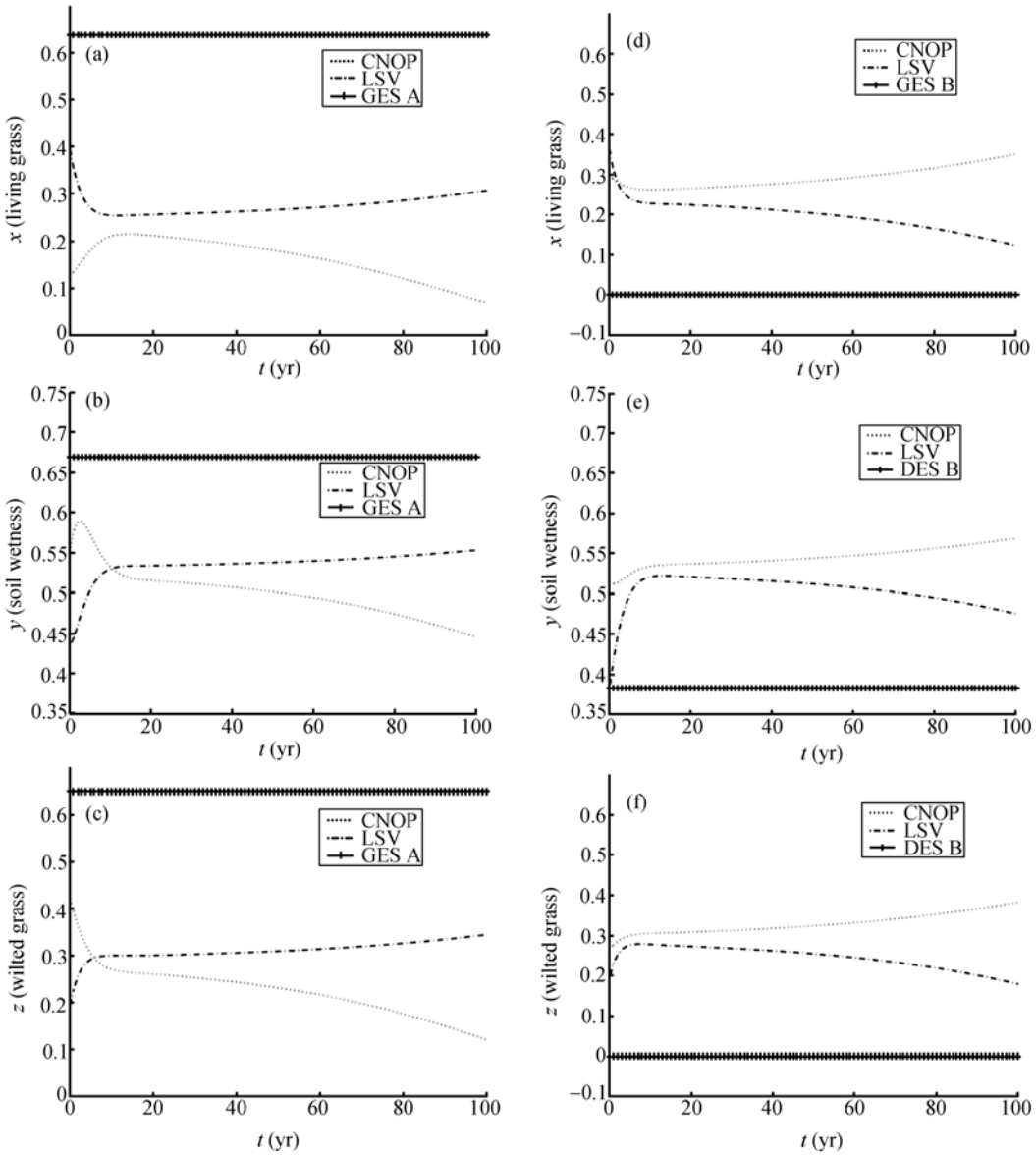


**Figure 14** Nonlinear evolutions of the ecosystem, left (right) column: a GES equilibrium state A (a DES equilibrium state B) plus CNOPs and LSVs as the initial conditions with $\delta$=0.57 ($\delta$=0.42). For the same magnitude, CNOPs yield a transition but LSVs does not. This figure is from ref. [58].

servation[66]. However, due to the limitation of linearity of SV, the initial perturbation fields of ensemble forecast constructed by LSVs may not be better to describe the real initial uncertainties; meanwhile, the sensitive area determined by LSV could also remain questionable. Since CNOP is directly from a nonlinear model and is concerned with the effect of nonlinearity, it could be a better candidate than LSV in yielding the initial perturbation fields of ensemble forecast and identifying sensitive area of target observation. In fact, the works of Mu and Jiang[67] on ensemble forecast and Mu et al.[68] on target observation supports this argument. The details are as follows.

### 5.1 Ensemble forecasting

One of the key problems in ensemble prediction is the generation of initial ensemble perturbations, which is expected to reflect the real initial uncertainty. At the European Centre for Medium-Range Weather Forecasts (ECMWF), the LSV approach has been successfully applied to generating initial perturbations for ensemble forecasting. However, as mentioned above, the linear theory of SV could not guarantee the optimal of a nonlinear system. Considering this point, Mu and Jiang[67] use CNOP to construct the initial perturbation fields of ensemble forecasting, in attempt to remedy the

limitation of SV and then improve the forecast skill.

Under a perfect model assumption, Mu and Jiang[67] demonstrated that the ensemble forecast skill may depend on the type of the analysis error when using CNOP method. When the analytical error is fast-growing type, the CNOP-type initial perturbation field, which is obtained by replacing the first SV of the perturbation field yielded by SVs with CNOP, causes better ensemble mean forecast than the SV-type initial perturbation field composed of SVs does (Figure 15). Furthermore, with the reduction of the magnitudes of analysis error, the ensemble mean skill caused by the CNOP-type initial perturbation field approaches gradually that caused by the SV-type initial perturbation field. This indicates that CNOP-type initial perturbation field could capture more effectively the characteristic of the fast-growing type of analytical errors, and consequently makes the ensemble forecast better. When the analytical error is slowly-growing type, the Monte Carlo method can provide a good forecast, whereas the ensembles mean of the CNOP- and SV-type initial perturbation field makes the forecast worse (Figure 15).

From these results, it is suggested that by introducing CNOP in ensemble forecast, it is hopeful to improve the forecast skill although it depends on the type of analytic errors. This work is a preliminary exploration of the CNOP method to ensemble prediction since there only one CNOP is used as ensemble perturbations. If one further investigates the application of CNOP to ensemble forecasts, more complex models and a large number of experiments should be used to confirm the above results. CNOPs of different initial constraint conditions and/or different optimization time should also be applied in the ensemble forecasts, and especially the local CNOP of some basic states need to be explored. It is expected that a more effective strategy of constructing ensemble initial perturbation field related to CNOP can be designed to serve the realistic ensemble forecast.

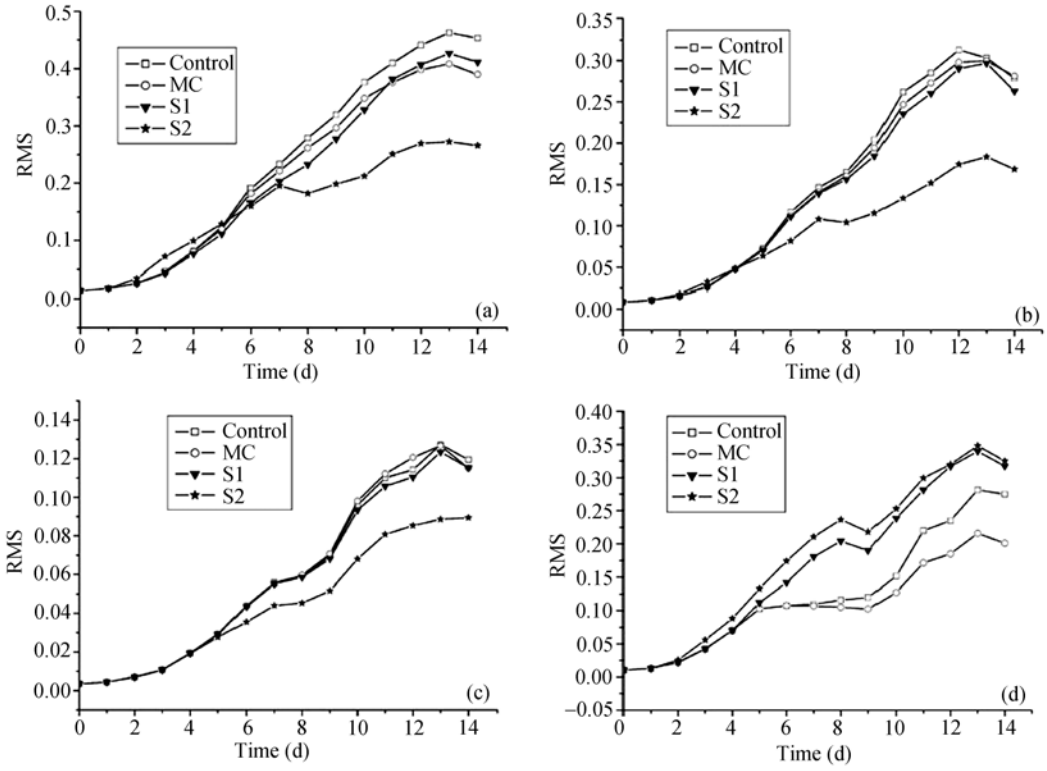


**Figure 15** Comparisons of the Root Mean Squared (RMS) skills of the ensemble mean forecasts with initial perturbation fields yielded by Monte Carlo method (denoted by "MC" in this figure), SV method (denoted by "S1"), and CNOP method (denoted by "S2"). The "control" in the figure signifies the control forecast. The horizontal axis represents the forecast time. (a), (b), and (c) correspond to the fast-growing analytical errors with energy norm as 0.0664, 0.0340, and 00158. In this case, CNOP method provides a better forecast of ensemble mean. With the reduction of the amplitude of analytical error, the RMS skill difference between CNOP and SV methods becomes gradually small. (d) Corresponds to the slowly-growing analytical error. In this case, Monte Carlo method can improve the forecast skill a little. This figure is from ref. [67].

### 5.2 Target observation

Target observation, which places observations in specific regions (sensitive areas) according to weather or climate events such as tropical cyclones, precipitation, etc., is another important technique that is used to improve the predictability. Palmer et al.[66] first applied LSV approach in target observation. Due to the limitation of LSV approximation, the sensitive area determined by LSV may be questionable. It is necessary to use a nonlinear technique for determining the sensitive area in target observation. Therefore, Mu et al.[68] investigated primarily the application of CNOP in target observation for precipitations.

In ref. [68], Mesoscale model 5 (MM5) and its adjoint were utilized to determine the sensitive area of precipitations. Two precipitation cases in July 2003 and August 1996 were adopted. The authors compared the structures between the CNOP and the first SV related to the two precipitation cases, and investigated the development of their total energies. They found that the structures of the CNOPs are considerably different from those of the first SV (Figure 16), as well as the evolutions of their total energies. On the basis of these results, some sensitivity experiments were performed in ref. [68]. It was found that the forecast results on these two precipitation cases are more sensitive to the CNOP type errors than the first SV type ones (Figure 17). Furthermore, CNOP-type errors have a more localized area and show a different signs from those of first SV. CNOP is directly based on a nonlinear model and not a linear approximation. Therefore, it is more accountable to use CNOP for identifying sensitive area of target observation. These suggest that the spatial pattern of CNOP type errors could be potential better than first SV for capturing the sensitive area.

Although the work of Mu et al.[68] is preliminary, it provides an important step for applying further CNOP in determining sensitive area. Of course, it requires a large of cases for examining the argument of CNOP being superior to first SV in determining sensitive area. Furthermore, it is expected that the method that determines the sensitive area by using CNOP's and LSV's spatial patterns can be presented in future papers. It is also expected that hindcast experiments will be performed to examine the effectiveness of the sensitive area determined by CNOP.

The above two studies apply firstly CNOP method to ensemble forecast and target observation, respectively.

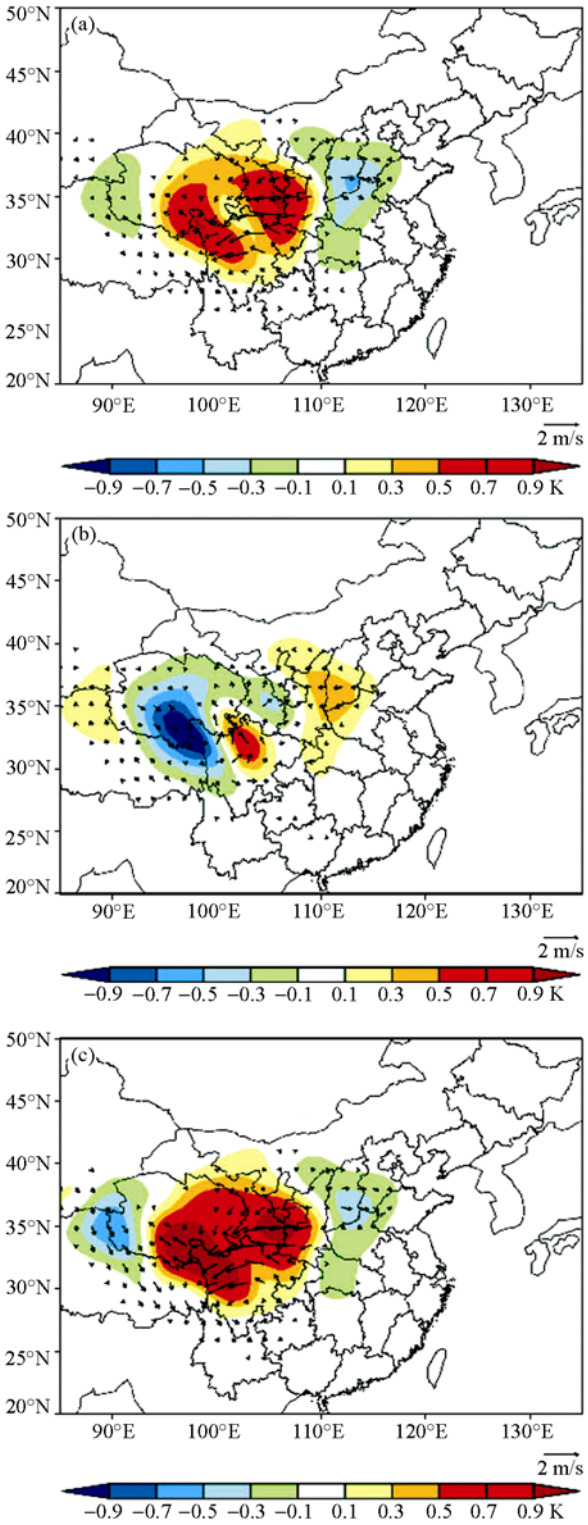


**Figure 16** Temperature (shaded) and wind vector at level $\sigma = 0.45$ for the precipitation that occurs from 00 UTC July 4, 2003 to 00 UTC July 5, 2003. They are respectively the components of CNOP-type error (a), FSV-type error (b), local CNOP type error (c). Their patterns are different. The forecast result of this precipitation is most sensitive to CNOP-type error. CNOP is more applicable than FSV in determining the sensitive area of target observation. This figure is from ref. [68].

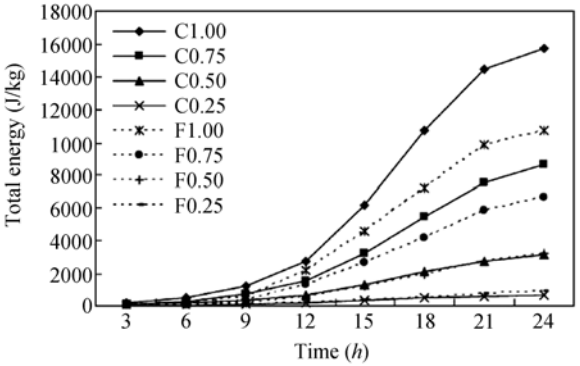


**Figure 17** The development of total energy sensitivity trials C1.00 (F1.00), C0.75 (F0.75), C0.50 (F0.50), C0.25 (F0.25), where C (F) represents CNOP (FSV) and the subsequent number (denoted by "*r*") means that the magnitudes of CNOP (FSV) are reduced with an amplitude of (1–*r*). The development of total energy is more sensitive to CNOP pattern than FSV pattern. This figure is from ref. [68].

Although this is an attempt, the information provided by the resultant results is exciting. Furthermore, given the nonlinear essence of atmosphere and ocean and the nonlinearity of CNOP, it is reasonable that to explore CNOP's applications to ensemble forecast and target observation is a useful research subject. We hope that scientists can be interested in these works and encourage the studies of CNOP's applications to ensemble and target observation.

## 6 Summary and discussion

This paper reviews the conditional nonlinear optimal perturbation (CNOP) and its recent applications in stability and sensitivity analysis and predictability studies. CNOP represents the initial perturbation that satisfies certain constraint condition and has the largest nonlinear evolution at prediction time. CNOP has three intrinsic characteristics: (1) CNOP is considerably different from LSV for the large initial perturbations or/and long optimization time intervals. This difference exists not only in the patterns of CNOP and LSV, but also in their evolutions. (2) In some cases, there exist local CNOPs of clear physical physical meaning. (3) CNOP always locates the boundary of the constraint. These characteristics were also examined in more realistic models. Especially, the third characteristic has been proved theoretically. This theoretical analysis establishes the accountability of numerical computations of CNOP and encourages us to modify the existing optimization algorithms, in attempt to reduce the computation cost for CNOP.

The recent applications of CNOP in stability, sensitivity, and predictability enrich the physics of CNOP and make CNOP theory more substantial. CNOP is more applicable than LSV in revealing the effect of nonlinearity. CNOP can be applied not only in predictability studies but also in the nonlinear characteristic of the evolutions of atmosphere, ocean, and the interaction between them. Even for the more broad coupled systems, CNOP could also be a useful tool in exploring their predictabilities and nonlinear evolutions. CNOP, rather than LSV, represents the optimal precursors for a weather or climate event; in predictability studies, CNOP stands for the initial error that has the largest negative effect on prediction; and in sensitivity analysis, CNOP is the most unstable (sensitive) mode. Besides, we notice that in the sensitivity analysis of ecosystem reviewed in section 4, CNOP was used to investigate the problem of transition between equilibrium states. In this situation, CNOP represents the initial perturbation that most probably induces the transition between equilibrium states. Especially, the major breakthrough of CNOP's applications is the utilization of CNOP in ensemble forecast and target observation. The preliminary results have showed the applicability of CNOP in yielding initial perturbation field for ensemble forecasting and in determining the sensitive area of target observation. CNOP has also been adopted by scientist abroad to tackle the problems related to predictability. From the works reviewed in this paper, it is obvious that CNOP method has been gradually recognized and adopted by international scholars and has been applied to the studies of stability, sensitivity, and predictability.

In CNOP's recent applications, we further notice that the usefulness of CNOP involves the studies of the dynamics for atmospheric, oceanic, and a coupled ENSO system. It is well known that coupled systems are more popular in describing nature. The application of CNOP in coupled ENSO system suggests that CNOP could be applicable in investigating the nonlinear characteristic of the evolution of all coupled systems. Besides, as the aforementioned, CNOP was preliminarily used to explore the transition between equilibrium states. In fact, this is a typical nonlinear property. On the studies of multi-equilibrium regime for geophysical fluid dynamics, Chao et al.[62,63] have has done a great deal of significative works. CNOP, as a finite amplitude initial perturbation, is directly from nonlinear model and features the nonlinearity. The preliminary results have shown that CNOP can capture the initial perturbation that most

probably causes the transition between equilibrium states. As such, by using CNOP, one can obtain the critical value of the amplitude of the initial perturbations that cause a transition between equilibrium states. This critical value also gives the boundary of the amplitude of initial perturbation that causes nonlinearly unstable. It is obvious that CNOP is useful in studying multi-equilibrium regime and even the nonlinear characteristic of the evolution of atmospheric, oceanic, and coupled systems.

To sum up, CNOP possesses particular characteristics and then clear physical meanings, which are different from those of LSV and favor the application of CNOP to revealing the nonlinear characteristic of the evolution of atmospheric, oceanic, and coupled systems and exploring the effect of nonlinearity on stability, sensitivity, and predictability.

The motions of atmosphere and ocean and the interaction between them are very complex. The studies of the involved nonlinear dynamics and predictability are therefore especially challenging. With the development of the dynamics studies of atmosphere, ocean and coupled systems, scientists have made great progresses in weather forecast and climate prediction, especially the successful weather forecast and short term climate prediction. Despite such progresses, predictability studies are still a field of challenge. We expect that, through the in-depth collaboration of applied mathematician and meteorologist and the development of more powerful computers, significant progresses will be further made in the future, in which CNOP approach is expected to play an important role. Furthermore, we hope that CNOP method serves effectively the studies of atmospheric, oceanic, and coupled system dynamics, and further improves the predictability of them.


1 Tennekes H. Karl Popper and the accountability of numerical forecasting. ECMWF Workshop Proceedings. New Developments in Predictability. London: European Centre for Medium-Range Weather Forecasts, 1991
2 Thompson P. Uncertainty of the initial state as a factor in the predictability of large scale atmospheric flow patterns. Tellus, 1957, 9: 275－295
3 Palmer T N, Molteni F, Mureau R, et al. Ensemble prediction. ECMWF Res Department Tech Memo, 1992, 188: 45
4 Toth Z, Kalnay E. Ensemble forecasting at NMC: The generation of perturbations. Bull Amer Meteor Soc, 1993, 74: 2317－2330
5 Mu M, Zhang Z Y. Conditional nonlinear optimal perturbations of a two-dimensional quasigeostrophic model. J Atmos Sci, 2006, 63: 1587－1604
6 Moore A M, Kleeman R. The dynamics of error growth and predictability in a coupled model of ENSO. Q J R Meteorol Soc, 1996, 122: 1405－1446
7 Samelson R G, Tziperman E. Instability of the chaotic ENSO: The growth-phase predictability barrier. J Atmos Sci, 2001, 58: 3613－3625
8 Duan W S, Mu M. Application of nonlinear optimization method to quantifying the predictability of a numerical model for El Nino-Southern Oscillation. Prog Nat Sci, 2005, 15(10): 915－921
9 Mu M, Duan W S, Wang B. Season-dependent dynamics of nonlinear optimal error growth and El Nino-Southern Oscillation predictability in a theoretical model. J Geophys Res, 2007, 112: D10113, doi: 10.1029/2005JD006981
10 Mu M, Xu H, Duan W S. A kind of initial errors related to "spring predictability barrier" for El Nino events in Zebiak-Cane model. Geophys Res Lett, 2007, 34: L03709, doi: 0.1029/2006GL027412
11 Smith L A, Ziehmann C, Fraedrich K. Uncertainty dynamics and predictability in chaotic systems. Q J R Meteorol Soc, 1999, 125: 2855－2886
12 Lorenz E N. A study of the predictability of a 28-variable atmospheric model. Tellus, 1965, 17: 321－333
13 Xue Y, Cane M A, Zebaik S E. Predictability of a coupled model of ENSO using singular vector analysis. Part I: Optimal growth in seasonal background and ENSO cycles. Mon Weather Rev, 1997, 125: 2043－2056
14 Buizza R, Molteni F. The role of finite-time barotropic instability during the transition to blocking. J Atmos Sci, 1996, 53: 1675－1697
15 Frederisen J S. Adjoint sensitivity and finite time normal mode disturbances during blocking. J Atmos Sci, 1997, 47: 2409－2416
16 Tziperman E, Ioannou P J. Transient growth and optimal excitation of thermohaline variability. J Phys Oceanogr, 2002, 32: 3427－3435
17 Mu M. Nonlinear singualr vectors and nonlinear singular values. Sci China Ser D-Earth Sci, 2000, 43(4): 375－385
18 Mu M, Duan W S, Wang B. Conditional nonlinear optimal perturbation and its applications. Non Proc Geophys, 2003, 10: 493－501
19 Mu M, Wang J C. Nonlinear fastest growing perturbation and the first kind of predictability. Sci China Ser D-Earth Sci, 2001, 44(12): 1128－1139
20 Mu M, Duan W S. Conditional nonlinear optimal perturbation and its applications to the studies of weather and climate predictability. Chin Sci Bull, 2005, 50: 2401－2407
21 Mu M, Duan W S, Xu H, et al. Applications of conditional nonlinear optimal perturbation in predictability study and sensitivity analysis of weather and climate. Adv Atmos Sci, 2006, 23(6): 992－1002
22 Duan W S, Mu M, Wang B. Conditional nonlinear optimal perturbation as the optimal precursors for ENSO events. J Geophys Res, 2004, 109: D23105
23 Mu M, Sun L, Henk D A. The sensitivity and stability of the ocean's thermocline circulation to finite amplitude freshwater perturbations. J Phys Oceanogr, 2004, 34: 2305－2315
24 Sun L, Mu M, Sun D J, et al. Passive mechanism decadal variation of thermohaline circulation. J Geophys Res, 2005, 110: C07025, doi: 10.1029/2005JC002897
25 Liu Y M. Maximum principle of conditional nonlinear optimal

perturbation (in Chinese). J East Chin Norm Univ (Nat Sci), 2008, (2): 131－134
26 Riviere O, Lapeyre G, Talagrand O. Nonlinear generalization of singular vectors: Behavior in a baroclinic unstable flow. J Atmos Sci, 2008, 65: 1896－1911
27 Terwisscha van Scheltinga A D. Data assimilation with implicit ocean models. PhD dissertation. Utrecht: Institute for Marine and Atmospheric Research, Utrecht University, 2007. 119
28 Powell M J D. VMCWD: A Fortran subroutine for constrained optimization. Acm Sigmap Bull, 1983, 32: 4－16
29 Birgin E G, Martinez J M, Raydan M. Nonmonotone spectral projected gradient methods for convex sets. Siam J Opt, 2000, 10(4): 1196－1211
30 Jiang Z N, Mu M, Wang D H. Conditional nonlinear optimal perturbation of a T21L3 quasi-geostrophic model. Q J R Meteorol Soc, 2008, 134: 1027－1038
31 Rex D F. Blocking action in the middle troposphere and its effects upon regional climate. I: An aerological study of blocking action. Tellus, 1950, 2: 196－211
32 Molteni F, Palmer T N. Predictability and finite-time instability of the northern winter circulation. Quart J Roy Meteor Soc, 1993, 119: 269－298
33 Buizza R, Molteni F. The role of finite-time barotropic instability during the transition to blocking. J Atmos Sci, 1996, 53: 1675－1697
34 Frederiksen J S. Singular vector, finite-time normal modes, and error growth during blocking. J Atmos Sci, 2000, 57: 312－333
35 Mu M, Jiang Z N. A method to find out the perturbations triggering the blocking onset: Conditional nonlinear optimal perturbations. J Atmos Sci, 2008, 65: 3935－3946
36 Jin F F, An S I, Timmermann A, et al. Strong El Nino events and nonlinear dynamical heating. Geophys Res Lett, 2003, 30: 1120, doi: 10.1029/2002GL016356
37 An S I, Jin F F. Nonlinearity and asymmetry of ENSO. J Clim, 2004, 17: 2399－2412
38 Wang B, An S I. Why the properties of El Nino changed during the late 1970s. Geophys Res Lett, 2001, 28: 3709－3712
39 Duan W S, Mu M. Investigating decadal variability of El Nino-Southern Oscillation asymmetry by conditional nonlinear optimal perturbation. J Geophys Res, 2006, 111: C07015, doi: 10.1029/2005JC003458
40 Philander S G H. El Nino Southern Oscillation phenomena. Nature, 1983, 302: 295
41 Jin F F. An equatorial ocean recharge paradigm for ENSO. Part I: Conceptual model. J Atmos Sci, 1997, 54: 811－829
42 Rodgers K B, Friederichs P, Latif M. Tropical Pacific decadal variability and its relation to decadal modulations of ENSO. J Clim, 2004, 17: 3761－3774
43 Duan W S, Xu H, Mu M. Decisive role of nonlinear temperature advection in El Nino and La Nina amplitude asymmetry. J Geophys Res, 2008, 113: C01014, doi: 10.1029/2006JC003974
44 Wang B, Fang Z. Chaotic oscillation of tropical climate: A dynamic system theory for ENSO. J Atmos Sci, 1996, 53: 2786－2802
45 Zebiak S E, Cane A. A model El Nino-Southern Oscillation. Mon Weather Rev, 1987, 115: 2262－2278
46 Webster P J, Yang S. Monsoon and ENSO: Selectively interactive systems, Q J R Meteorol Soc, 1992, 118: 877－926
47 Wang C, Picaut J. Understanding ENSO physics—A review. In: Wang C Z, Xie S P, Carton J A, eds. Earth's Climate: The Ocean-Atmosphere Interaction. Geophys Monogr, 2004, 147: 21－48
48 Chen D, Cane M A, Kaplan A, et al. Predictability of El Nino over the past 148 years. Nature, 2004, 428: 733－736
49 Charney J G. The dynamics of long waves in a baroclinic westerly current. J Meteor, 1947, 4: 135－162
50 Eady E T. Long waves and cyclone waves. Tellus, 1949, 1: 33－52
51 Farrell B F. The initial growth of disturbances in baroclinic flows. J Atmos Sci, 1982, 39: 1663－1686
52 Lacarra J F, Talagrand O. Short-range evolution of small perturbations in a barotropic model. Tellus, 1988, 40: 81－95
53 Badger J, Hoskins B J. Simple initial value problems and mechanisms for baroclinic growth. J Atmos Sci, 2001, 58: 38－49
54 Jiang S, Jin F F, Ghil M. Multiple equilibria and aperiodic solutions in a wind-driven doublegyre, shallow-water model. J Phys Oceanogr, 1995, 25: 764－786
55 Dijkstra H A. Nonlinear Physical Oceanography: A Dynamical Systems Approach to the Large Scale Ocean Circulation and El Nino. 2nd ed. Dordrecht: Springer, 2005
56 Dijkstra H A, De Ruijter W P M. Finite amplitude stability of the wind-driven ocean circulation. Geophys Astrophys Fluid Dyn, 1996, 83: 1－31
57 Wu X G, Mu M. Impact of horizontal diffusion on the nonlinear stability of thermohaline circulation in a modified box model. J Phys Ocenogr, 2009, 39: 798－805
58 Mu M, Wang B. Nonlinear instability and sensitivity of a theoretical grassland ecosystem to finite-amplitude perturbations. Nonlinear Process Geophys, 2007, 14: 409－423
59 Zeng Q C, Lu P S, Zeng X D. Maximum simplified dynamic model of grass field ecosystem with two variables. Sci China Ser B, 1994, 37: 94－103
60 Zeng X D, Shen S H, Zeng X B, et al. Multiple equilibrium states and the abrupt transitions in a dynamical system of soil water interacting with vegetation. Geophys Res Lett, 2004, 31: 5501, doi: 10.1029/2003GL018910
61 Zeng Q C, Zeng X D. An analytical dynamic model of grass field ecosystem with two variables. Ecol Model, 1996, 85: 187－196
62 Chao J P, Zhang G K, Yuan X M. A preliminary investigation for the formation of pressure jump produced by the mountain in a two model (in Chinese). Acta Meteorol Sin, 1964, 34: 233－241
63 Chao J P. A preliminary analysis of the interaction between convection development and ambient environment (in Chinese). Acta Meteorol Sin, 1962, 32: 11－18
64 Houtekamer P L, Derome J. Methods for ensemble prediction. Mon Weather Rev, 1995, 123: 2181－2196
65 Hamill T M, Snyder C, Morss R E. A comparison of probabilistic forecasts from bred, singular-vector, and perturbed observation ensembles. Mon Weather Rev, 2000, 128: 1835－1851
66 Palmer T N, Gelaro R, Barkmeuer J, et al. Singular vectors, metrics, and adaptive observations. J Atmos Sci, 1998, 55: 633－653
67 Mu M, Jiang Z N. A new approach to the generation of initial perturbations for ensemble prediction: Conditional nonlinear optimal perturbation. Chin Sci Bull, 2008, 53(13): 2062－2068
68 Mu M, Wang H, Zhou F F. A preliminary application of conditional nonlinear optimal perturbation to adaptive observation (in Chinese). Chin J Atmos Sci, 2007, 31(6): 1102－1112